Electronic Supplementary Information (ESI)

Biomimetic hydrogen-bonding cascade for chemical activation: telling a nucleophile from a base

Hyunchang Park and Dongwhan Lee*

Department of Chemistry, Seoul National University, 1 Gwanak-ro, Gwanak-gu, Seoul 08826, Korea

Experimental Section

General Considerations. All reagents were obtained from commercial suppliers and used as received unless otherwise noted. The solvents DCM and THF were saturated with nitrogen and purified by passage through activated Al_2O_3 columns under nitrogen (Innovative Technology SPS PureSolv MD4). The solvent DMF was saturated with argon and purified by passage through activated Al_2O_3 columns under argon (Pure Process Technology GC-SPS-8). HPLC-grade H_2O was used for reactivity studies. The compounds 4-methylbenzo[*c*][1,2,5]thiadiazole,[1] benzo[*c*][1,2,5]thiadiazole-4-carbaldehyde,[2] 4-bromo-7-methylbenzo[*c*][1,2,5]thiadiazole,[3] 4-bromo-7-(bromomethyl)benzo[*c*][1,2,5]thiadiazole,[2] 4-bromo-7-(hydroxymethyl)benzo[*c*]thiadiazole,[4] 2-hydroxy-6-(methoxymethoxy)benzaldehyde,[5] and *N*-(phenyl(4,4,5,5-tetramethyl-1,3,2-dioxaborolan-2-yl)methyl)acetamide[6] were prepared according to literature procedures or their slight modifications. All air-sensitive manipulations were carried out under nitrogen atmosphere by standard Schlenk-line techniques.

Physical Measurements. ^{1}H NMR, ^{13}C NMR, 2D-COSY NMR, and 2D-ROESY NMR spectra were recorded on a Varian/Oxford As-500 (500 MHz) spectrophotometer, a JeolJNM-LA400 (400 MHz) spectrometer, an AVANCE 600 (600 MHz) spectrometer, and a 850 MHz Avance III HD Bruker NMR equipped with a TCI Cryoprobe. Variable-temperature ^{1}H NMR spectra were recorded on a JeolJNM-LA400 (400 MHz) spectrometer. Chemical shifts were reported versus tetramethylsilane, and referenced to the residual solvent peaks.[7] High-resolution ESI-MS spectra were obtained on a ESI-Q-TOF mass spectrometer (Compact, Bruker Daltonics Inc.,Bremen Germany). FT-IR spectra were recorded on a PerkinElmer Spectrum Two FT-IR Spectrometer. UV–vis spectra were recorded on an Agilent 8453 UV–vis spectrophotometer with ChemStation software. HPLC-MS analyses were performed on a Shimadzu Prominence LC-20A equipped with a SPD-20A UV detector, a Shim-pack GIS-ODS column (5 μm, size = 250 × 4.6 mm), and Labsolution software. Fluorescence

[1] R. Agneeswari, V. Tamilavan, M. Song and M. H. Hyun, *J. Mater. Chem. C.,* 2014, **2**, 8515–8524.
[2] R. Jonas, H. Prücher and H. Wurziger, *Eur. J. Med. Chem.,* 1993, **28**, 141–148.
[3] Y. Liu, M. Prashad and O. Repič, *J. Heterocyclic Chem.,* 2003, **40**, 713–716.
[4] S. Haid, M. Marszalek, A. Mishra, M. Wielopolski, J. Teuscher, J. Moser, R. Humphry-Baker, S. M. Zakeeruddin, M. Grätzel and P. Bäuerle, *Adv. Funct. Mater.,* 2012, **22**, 1291–1302.
[5] B. Metcalf, C. Chuang, K. Dufu, M. P. Patel, A. Silva-Garcia, C. Johnson, Q. Lu, J. R. Partridge, L. Patskovska, Y. Patskovsky, S. C. Almo, M. P. Jacobson, L. Hua, Q. Xu, S. L. Gwaltney, C. Yee, J. Harris, B. P. Morgan, J. James, D. Xu, A. Hutchaleelaha, K. Paulvannan, D. Oksenberg and Z. Li, *ACS. Med. Chem. Lett.,* 2017, **8**, 321–326
[6] T. Ohmura, T. Awano and M. Suginome, *Chem. Lett.,* 2009, **38**, 664–665
[7] G. R. Fulmer, A. J. M. Miller, N. H. Sherden, H. E. Gottlieb, A. Nudelman, B. M. Stoltz, J. E. Bercaw and K. I. Goldberg, *Organometallics,* 2010, **29**, 2176–2179.

spectra were recorded on a Photon Technology International (PTI) QM-400 spectrofluorometer with FelixGX software.

Job Plot Ananlysis of the Reaction Stoichiometry between 1 and Cyanide Ion. Solution samples of **1** and NaCN were prepared separately in DMSO (66.7 μM each), and mixed in various volume ratios (**1** only, 1:9, 2:8, 3:7, 4:6, 5:5, 6:4, 7:3, 8:2, 9:1, and NaCN only) to maintain a constant overall concentration of the combined components. The absorbance at $\lambda = 410$ nm was measured and plotted.

HPLC-MS Analysis of the Cyanohydrin Adduct of 1. A solution sample of **1** (0.333 mM) and NaCN (25 equiv) was prepared in DMSO (1.5 mL). A 5 μL aliquot was taken by the auto-sampler, and subjected to HPLC-MS analysis (MeCN–H_2O (9:1, v/v) containing 0.1% TFA as eluent). The MS spectrum at $t_R = 3.60$ min was recorded. Control studies with untreated **1** (0.333 mM in DMSO) produced a chromatogram at $t_R = 4.25$ min, which was confirmed by MS analysis.

Determination of the Rate Constant for the Reaction of 1 with Cyanide. Solution samples of **1** (40.0 μM) in DMSO–MeCN (1:1, v/v) were prepared, and treated with NaCN (10, 20, and 30 equiv) at 288 K with stirring (1200 rpm). After adding NaCN, changes in the absorbance at $\lambda = 400$ nm were recorded per 1 s. The experimental data points were fitted to the theoretical *pseudo*-first-order kinetic model to determine the rate constant, k'. The second-order rate constant was estimated by plotting k' vs $[CN^-]_0$, and obtaining a linear fit.

Scheme S1. Synthetic route to **2**.

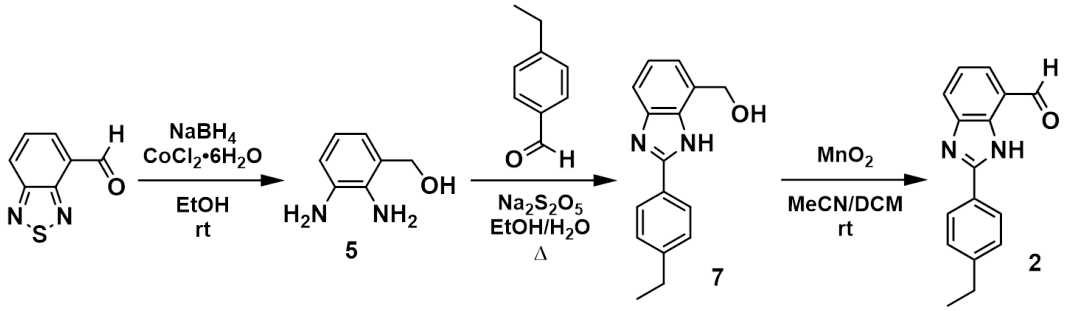

(2,3-Diaminophenyl)methanol (5). To a stirred EtOH (150 mL) suspension of benzo[*c*][1,2,5]thiadiazole-4-carbaldehyde[2] (1.36 g, 8.28 mmol) was added $CoCl_2{\cdot}6\,H_2O$ (356 mg, 1.50 mmol). The mixture was cooled to 0 °C, and $NaBH_4$ (3.14 g, 83.0 mmol) was added portionwise. The reaction mixture was warmed to r.t., stirred for 3 h, and quenched by adding water (150 mL). Insoluble material was removed by filtration, and the filtrate was extracted into EtOAc (200 mL × 3). The combined extracts were dried over anhyd $MgSO_4$, filtered, and concentrated under reduced pressure. Flash column chromatography on SiO_2 (hexane:EtOAc:MeOH = 5:5:1, v/v) furnished **5** as a pale yellow solid (416 mg, 3.01 mmol, yield = 36%). ^{1}H NMR (500 MHz, DMSO-d_6, 298 K): δ 6.47 (d, J = 7.5 Hz, 1H), 6.41 (d, J = 7.4 Hz, 1H), 6.35 (t, J = 7.5 Hz, 1H), 4.91 (t, J = 5.4 Hz, 1H), 4.42 (s, 2H), 4.36 (d, J = 5.4 Hz, 2H), 4.33 (s, 2H). ^{13}C NMR (125 MHz, DMSO-d_6, 298 K): δ 134.9, 132.9, 125.6, 117.3, 116.5, 114.1, 61.9. FT-IR (ATR, cm^{-1}): 3397, 3325, 3192, 3032, 2917, 2873, 1615, 1476, 1393, 1297, 1256, 1209, 1174, 1131, 1000, 916, 875, 780, 732, 691. HRMS (ESI) calcd for $C_7H_{10}N_2O$ $[M + H]^+$ 139.0866, found 139.0868.

(2-(4-Ethylphenyl)-1H-benzo[*d*]imidazol-7-yl)methanol (7). To a stirred solution of **5** (78.9 mg, 0.571 mmol) in EtOH (25 mL) was added 4-ethylbenzaldehyde (0.20 mL, 1.5 mmol). The solution was stirred for 10 min at 60 °C, and treated with an aq solution (0.7 mL) of $Na_2S_2O_5$ (90.8 mg, 0.478 mmol). The reaction mixture was heated at reflux for 12 h, cooled to r.t., and concentrated under reduced pressure. The crude mixture was diluted with EtOAc (100 mL), washed with water (100 mL), and extracted into EtOAc (100 mL × 2). The combined extracts were dried over anhyd $MgSO_4$, filtered, and concentrated under reduced pressure. Flash column chromatography on SiO_2 (hexane:EtOAc = 9:1 to 1:2, v/v) furnished **7** as a white solid (110 mg, 0.436 mmol, yield = 76%). ^{1}H NMR (400 MHz, DMSO-d_6, 343 K): δ 12.46 (s, 1H), 8.13 (d, J = 7.9 Hz, 2H), 7.47 (d, J = 7.0 Hz, 1H), 7.38 (d, J = 7.9 Hz, 2H), 7.24 (d, J = 7.2 Hz, 1H), 7.17 (t, J = 7.6 Hz, 1H), 4.95 (s, 2H), 2.70 (q, J = 7.5 Hz, 2H), 1.25 (t, J = 7.5 Hz, 3H). ^{13}C NMR (100 MHz, DMSO-d_6, 343 K): δ 150.9, 145.3, 127.8, 127.6, 126.4, 121.4, 119.5, 59.4, 27.7, 14.8.[8] FT-IR (ATR, cm^{-1}): 3054, 2960, 2930, 2859, 2817, 1744, 1718, 1622, 1502, 1481, 1433, 1373, 1318, 1292, 1269, 1237, 1162, 1112, 1059, 1016, 951, 839, 794, 744, 725, 697. HRMS (ESI) calcd for $C_{16}H_{16}N_2O$ $[M + H]^+$ 253.1335, found 253.1334.

2-(4-Ethylphenyl)-1H-benzo[*d*]imidazole-7-carbaldehyde (2). To a stirred solution of **7** (123 mg, 0.487 mmol) in MeCN–CH_2Cl_2 (4:1, v/v, 25 mL) was added MnO_2 (88% active, 510 mg, 5.16 mmol). The reaction mixture was stirred at r.t. for 4 h, diluted with CH_2Cl_2 (50 mL), and filtered through a bed of Celite. The filtrate was washed with a sat'd aq solution of $NaHCO_3$ (100 mL), and the residual organic fraction was extracted into CH_2Cl_2 (100 mL × 2). The combined

[8] The resonances of four aromatic carbons were not found due to tautomerization.

extracts were dried over anhyd $MgSO_4$, filtered, and concentrated under reduced pressure. Flash column chromatography on SiO_2 (hexane:EtOAc = 9:1 to 3:1, v/v) furnished **2** as a white solid (91.8 mg, 0.367 mmol, yield = 75%). ^{1}H NMR (500 MHz, $CDCl_3$, 298 K): δ 10.99 (s, 1H), 10.10 (s, 1H), 8.05 (d, J = 7.9 Hz, 1H), 8.02 (d, J = 7.9 Hz, 2H), 7.68 (d, J = 7.4 Hz, 1H), 7.39 (t, J = 7.7 Hz, 1H), 7.34 (d, J = 7.8 Hz, 2H), 2.71 (q, J = 7.6 Hz, 2H), 1.27 (t, J = 7.7 Hz, 3H). ^{13}C NMR (125 MHz, $CDCl_3$, 298 K): δ 192.7, 153.9, 147.5, 145.2, 133.0, 128.7, 128.4, 127.0, 126.7, 126.4, 122.3, 121.2, 28.9, 15.3. FT-IR (ATR, cm^{-1}): 3327, 3054, 2964, 2929, 2847, 2806, 2730, 1681, 1611, 1600, 1542, 1493, 1458, 1426, 1384, 1360, 1318, 1293, 1273, 1221, 1163, 1088, 1061, 1048, 1020, 966, 948, 882, 859, 831, 790, 736. HRMS (ESI) calcd for $C_{16}H_{14}N_2O$ $[M + H]^+$ 251.1179, found 251.1180.

Scheme S2. Synthetic routes to **3** and **4**.

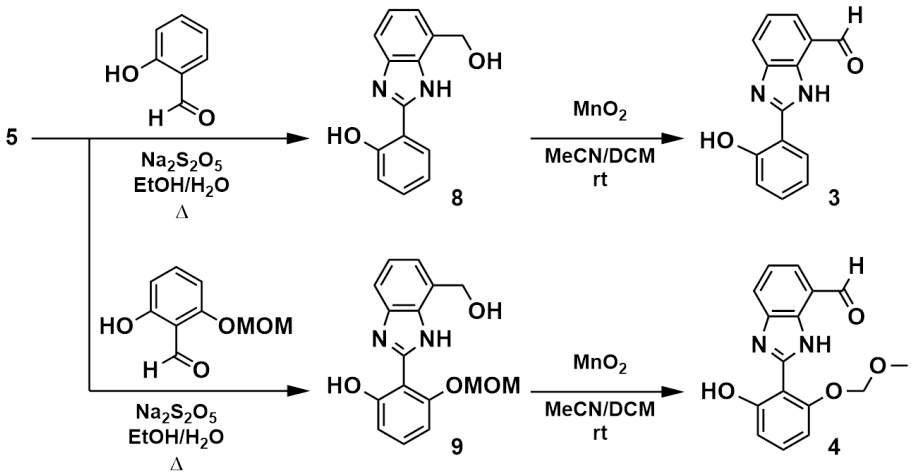

2-(7-(Hydroxymethyl)-1H-benzo[*d*]imidazol-2-yl)phenol (8). To a stirred solution of **5** (204 mg, 1.48 mmol) in EtOH (60 mL) was added salicylaldehyde (0.39 mL, 3.7 mmol). The solution was stirred for 10 min at 60 °C, and treated with an aq solution (2.0 mL) of $Na_2S_2O_5$ (235 mg, 1.24 mmol). The reaction mixture was heated at reflux for 12 h, cooled to r.t., and concentrated under reduced pressure. The crude mixture was diluted with EtOAc (100 mL), washed with water (100 mL), and extracted into EtOAc (100 mL × 2). The combined extracts were dried over anhyd $MgSO_4$, filtered, and concentrated under reduced pressure. Flash column chromatography on SiO_2 (hexane:EtOAc = 9:1 to 1:2, v/v) furnished **8** as a pale yellow solid (295 mg, 1.23 mmol, yield = 83%). ^{1}H NMR (500 MHz, CD_3OD, 298 K): δ 7.92 (d, J = 7.8 Hz, 1H), 7.48 (d, J = 7.8 Hz, 1H), 7.32–7.21 (m, 3H), 6.99 (d, J = 8.3 Hz, 1H), 6.94 (t, J = 7.5 Hz, 1H), 5.01 (s, 2H). ^{13}C NMR (125 MHz, CD_3OD, 298 K): δ 159.5, 153.0, 132.7, 132.5, 129.7, 128.3, 127.1, 124.1, 124.0, 122.1, 120.3, 118.2, 114.3, 61.6. FT-IR (ATR, cm^{-1}): 3356, 3183, 3130, 3068, 1630, 1598, 1538, 1487, 1420, 1403, 1322, 1257, 1167, 1134, 1069, 1034, 998, 969, 902, 872, 830, 795, 748, 691. HRMS (ESI) calcd for $C_{14}H_{12}N_2O_2$ $[M + H]^+$ 241.0972, found 241.0972.

2-(7-(Hydroxymethyl)-1H-benzo[*d*]imidazol-2-yl)-3-(methoxymethoxy)phenol (9). To a stirred solution of **5** (77.3 mg, 0.559 mmol) in EtOH (21 mL) was added 2-hydroxy-6-(methoxymethoxy)benzaldehyde[5] (257 mg, 1.41 mmol). The solution was stirred for 10 min at 60 °C, and treated with an aq solution (0.8 mL) of $Na_2S_2O_5$ (89.3 mg, 0.470 mmol). The reaction mixture was heated at reflux for 12 h, cooled to r.t., and concentrated under reduced pressure.

The crude mixture was diluted with EtOAc (100 mL), washed with water (100 mL), and extracted into EtOAc (100 mL × 2). The combined extracts were dried over anhyd $MgSO_4$, filtered, and concentrated under reduced pressure. Flash column chromatography on SiO_2 (hexane:EtOAc = 9:1 to 1:1, v/v) furnished **9** as a yellow solid (129 mg, 0.430 mmol, yield = 77%). ^{1}H NMR (500 MHz, CD_3OD, 298 K): δ 7.57 (dd, J = 6.1, 3.1 Hz, 1H), 7.31–7.14 (m, 3H), 6.76 (d, J = 8.4 Hz, 1H), 6.68 (d, J = 8.3 Hz, 1H), 5.47 (s, 2H), 5.04 (s, 2H), 3.53 (s, 3H). ^{13}C NMR (125 MHz, CD_3OD, 298 K): δ 161.8, 157.1, 151.3, 132.3, 129.5, 123.9, 121.6, 114.2, 112.2, 105.5, 104.1, 96.0, 62.2, 56.9.[9] FT-IR (ATR, cm^{-1}): 3456, 3421, 3065, 3005, 2864, 2830, 1622, 1593, 1524, 1478, 1445, 1404, 1380, 1318, 1277, 1238, 1202, 1151, 1091, 1072, 1034, 934, 920, 872, 843, 786, 737, 712, 657. HRMS (ESI) calcd for $C_{16}H_{16}N_2O_4$ $[M + H]^+$ 301.1183, found 301.1185.

2-(2-Hydroxyphenyl)-1H-benzo[*d*]imidazole-7-carbaldehyde (3). To a stirred solution of **8** (74.6 mg, 0.310 mmol) in MeCN–CH_2Cl_2 (4:1, v/v, 15 mL) was added MnO_2 (88% active, 324 mg, 3.28 mmol). The reaction mixture was stirred at r.t. for 7 h, diluted with CH_2Cl_2 (50 mL), and filtered through a bed of Celite. The filtrate was washed with a sat'd aq solution of $NaHCO_3$ (100 mL), and the residual organic fraction was extracted into CH_2Cl_2 (100 mL × 2). The combined extracts were dried over anhyd $MgSO_4$, filtered, and concentrated under reduced pressure. Flash column chromatography on SiO_2 (hexane:EtOAc = 9:1 to 4:1, v/v) furnished **3** as a white solid (44.7 mg, 0.188 mmol, yield = 61%). ^{1}H NMR (500 MHz, CD_3OD, 298 K): δ 10.30 (s, 1H), 8.22–8.16 (m, 1H), 7.99 (d, J = 8.2 Hz, 1H), 7.86 (d, J = 7.7 Hz, 1H), 7.49 (t, J = 7.8 Hz, 1H), 7.40 (t, J = 7.7 Hz, 1H), 7.09–6.98 (m, 2H), 4.60 (s, 1H). ^{13}C NMR (100 MHz, DMSO-d_6, 343 K): δ 190.6, 157.6, 153.3, 131.9, 127.2, 124.2, 122.2, 118.9, 116.9, 112.5.[10] FT-IR (ATR, cm^{-1}): 3301, 3067, 2922, 2842, 1673, 1632, 1590, 1527, 1486, 1440, 1418, 1390, 1370, 1324, 1282, 1256, 1218, 1205, 1170, 1084, 1064, 1041, 958, 940, 886, 835, 796, 760, 744, 716, 667. HRMS (ESI) calcd for $C_{14}H_{10}N_2O_2$ $[M + H]^+$ 239.0815, found 239.0817.

2-(2-Hydroxy-6-(methoxymethoxy)phenyl)-1H-benzo[*d*]imidazole-7-carbaldehyde (4). To a stirred solution of **9** (158 mg, 0.526 mmol) in MeCN–CH_2Cl_2 (4:1, v/v, 25 mL) was added MnO_2 (88% active, 627 mg, 6.35 mmol). The reaction mixture was stirred at r.t. for 20 h, diluted with CH_2Cl_2 (100 mL), and filtered through a bed of Celite. The filtrate was washed with water (100 mL), and the residual organic fraction was extracted into CH_2Cl_2 (100 mL × 2). The combined extracts were dried over anhyd $MgSO_4$, filtered, and concentrated under reduced pressure. Flash column chromatography on SiO_2 (hexane:EtOAc = 9:1 to 3:1, v/v) furnished **4** as a yellow solid (124 mg, 0.416 mmol, yield = 79%). ^{1}H NMR (500 MHz, $CDCl_3$, 298 K): δ 13.80 (s, 1H), 11.89 (s, 1H), 10.04 (s, 1H), 7.89 (d, J = 8.0 Hz, 1H), 7.61 (d, J = 7.4 Hz, 1H), 7.33 (t, J = 7.7 Hz, 1H), 7.18 (t, J = 8.3 Hz, 1H), 6.71 (d, J = 8.3 Hz, 1H), 6.61 (d, J = 8.3 Hz, 1H), 5.42 (s, 2H), 3.59 (s, 3H). ^{13}C NMR (125 MHz, $CDCl_3$, 298 K): δ 192.3, 161.2, 155.7, 152.7, 141.2, 132.2, 130.3, 128.4, 124.8, 122.6, 121.1, 111.9, 104.0, 102.5, 95.4, 57.3. FT-IR (ATR, cm^{-1}): 3445, 3085, 2913, 2832, 2744, 1666, 1591, 1523, 1474, 1448, 1407, 1388, 1364, 1308, 1273, 1240, 1196, 1152, 1090, 1077, 1037, 944, 918, 884, 839, 792, 777, 741, 723. HRMS (ESI) calcd for $C_{16}H_{14}N_2O_4$ $[M + H]^+$ 299.1026, found 299.1029.

[9] The resonances of two aromatic carbons were not found due to tautomerization.
[10] The resonances of four aromatic carbons were not found due to tautomerization.

Scheme S3. Synthetic route to **1**.

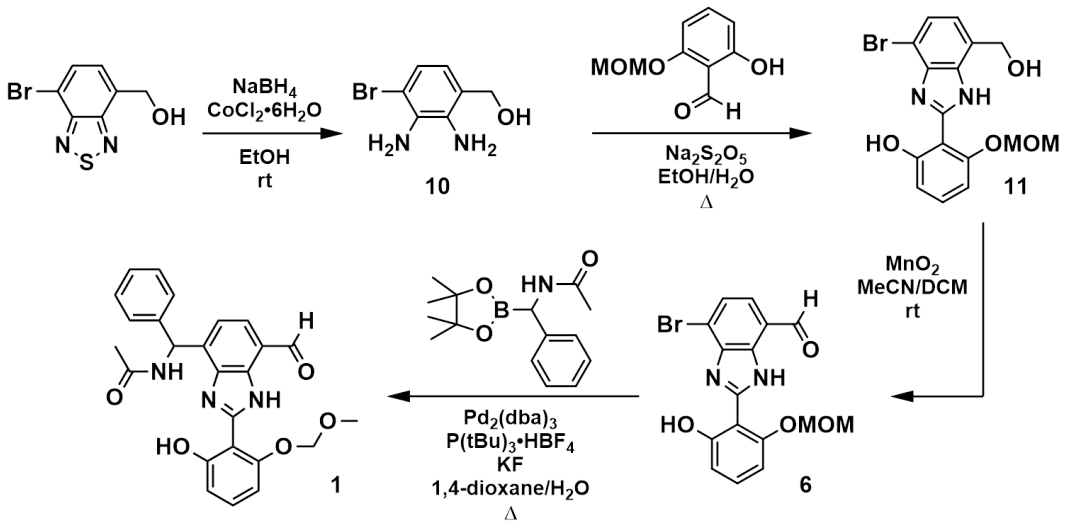

(2,3-Diamino-4-bromophenyl)methanol (10). To a stirred EtOH (50 mL) suspension of 4-bromo-7-(hydroxymethyl)benzo[*c*]thiadiazole[4] (905 mg, 3.69 mmol) was added $CoCl_2 \cdot 6\,H_2O$ (159 mg, 0.668 mmol). The mixture was cooled to 0 °C, and $NaBH_4$ (1.41 g, 37.3 mmol) was added portionwise. The reaction mixture was warmed to r.t., stirred for 2 h, and quenched by adding water (150 mL). Insoluble material was removed by filtration, and the filtrate was extracted into EtOAc (200 mL × 3). The combined extracts were dried over anhyd $MgSO_4$, filtered, and concentrated under reduced pressure. Flash column chromatography on SiO_2 (hexane:EtOAc = 9:1 to 1:3, v/v) furnished **10** as a pale yellow solid (566 mg, 2.61 mmol, yield = 71%). ^{1}H NMR (500 MHz, DMSO-d_6, 298 K): δ 6.67 (d, J = 8.2 Hz, 1H), 6.41 (d, J = 8.2 Hz, 1H), 5.02 (t, J = 5.4 Hz, 1H), 4.70 (s, 2H), 4.63 (s, 2H), 4.36 (d, J = 5.1 Hz, 2H). ^{13}C NMR (125 MHz, DMSO-d_6, 298 K): δ 133.8, 131.8, 124.6, 119.3, 117.9, 107.6, 61.2. FT-IR (ATR, cm^{-1}): 3379, 3302, 3226, 1592, 1471, 1449, 1279, 1249, 1204, 1140, 989, 938, 855, 796, 761, 710. HRMS (ESI) calcd for $C_7H_9BrN_2O$ $[M + H]^+$ 216.9971, found 216.9968.

2-(4-Bromo-7-(hydroxymethyl)-1H-benzo[*d*]imidazol-2-yl)-3-(methoxymethoxy)-phenol (11). To a stirred solution of **10** (566 mg, 2.61 mmol) in EtOH (90 mL) was added 2-hydroxy-6-(methoxymethoxy)benzaldehyde[5] (702 mg, 3.85 mmol). The solution was stirred for 10 min at 60 °C, and treated with an aq solution (3.6 mL) of $Na_2S_2O_5$ (415 mg, 2.18 mmol). The reaction mixture was heated at reflux for 16 h, cooled to r.t., and concentrated under reduced pressure. The crude mixture was diluted with EtOAc (100 mL), washed with water (100 mL), and extracted into EtOAc (100 mL × 2). The combined extracts were dried over anhyd $MgSO_4$, filtered, and concentrated under reduced pressure. Flash column chromatography on SiO_2 (hexane:EtOAc = 9:1 to 1:3, v/v) furnished **11** as a pale yellow solid (866 mg, 2.28 mmol, yield = 87%). ^{1}H NMR (500 MHz, DMSO-d_6, 298 K): δ 13.80 (s, 1H), 11.84 (s, 1H), 7.46 (d, J = 7.9 Hz, 1H), 7.34 (t, J = 8.3 Hz, 1H), 7.11 (d, J = 7.9 Hz, 1H), 6.78 (d, J = 8.3 Hz, 1H), 6.73 (d, J = 8.3 Hz, 1H), 5.82 (t, J = 5.0 Hz, 1H), 5.48 (s, 2H), 4.94 (d, J = 4.9 Hz, 2H), 3.49 (s, 3H). ^{13}C NMR (125 MHz, DMSO-d_6, 298 K): δ 159.9, 155.2, 150.0, 138.3, 132.1, 130.7, 126.0, 124.9, 121.4, 110.8, 108.1, 104.5, 102.1, 95.0, 61.0, 56.5. FT-IR (ATR, cm^{-1}): 3436, 2959, 2927, 2906, 2830, 1624, 1592, 1524, 1472, 1401, 1373, 1312, 1273, 1241, 1202, 1156, 1115, 1090, 1073, 1026, 928, 807, 791, 778, 749, 728. HRMS (ESI) calcd for $C_{16}H_{15}BrN_2O_4$ $[M + H]^+$ 379.0288, found 379.0286.

4-Bromo-2-(2-hydroxy-6-(methoxymethoxy)phenyl)-1H-benzo[*d*]imidazole-7-carbaldehyde (6). To a stirred solution of **11** (866 mg, 2.28 mmol) in MeCN–CH_2Cl_2 (11:3, v/v, 140 mL) was added MnO_2 (88% active, 2.71 g, 27.4 mmol). The reaction mixture was stirred at r.t. for 20 h, diluted with CH_2Cl_2 (100 mL), and filtered through a bed of Celite. The filtrate was washed with water (150 mL), and the residual organic fraction was extracted into CH_2Cl_2 (150 mL × 2). The combined extracts were dried over anhyd $MgSO_4$, filtered, and concentrated under reduced pressure. Flash column chromatography on SiO_2 (hexane:EtOAc = 3:1 to 2:1, v/v) furnished **6** as a pale yellow solid (715 mg, 1.90 mmol, yield = 83%). ^{1}H NMR (500 MHz, $CDCl_3$, 298 K): δ 13.47 (s, 1H), 11.97 (s, 1H), 10.01 (s, 1H), 7.49 (d, J = 7.9 Hz, 1H), 7.45 (d, J = 7.9 Hz, 1H), 7.20 (t, J = 8.3 Hz, 1H), 6.71 (d, J = 8.4 Hz, 1H), 6.60 (d, J = 8.3 Hz, 1H), 5.43 (s, 2H), 3.60 (s, 3H). ^{13}C NMR (125 MHz, $CDCl_3$, 298 K): δ 191.6, 161.3, 155.8, 153.0, 140.4, 132.7, 130.3, 128.7, 125.8, 120.2, 119.8, 112.1, 104.1, 102.1, 95.5, 57.4. FT-IR (ATR, cm^{-1}): 3429, 3063, 3025, 2959, 2909, 2820, 2720, 1677, 1633, 1585, 1521, 1471, 1412, 1381, 1354, 1344, 1312, 1265, 1242, 1199, 1154, 1118, 1090, 1080, 1033, 940, 922, 809, 787, 739, 658. HRMS (ESI) calcd for $C_{16}H_{13}BrN_2O_4$ $[M + H]^+$ 377.0132, found 377.0136.

***N*-((7-Formyl-2-(2-hydroxy-6-(methoxymethoxy)phenyl)-1H-benzo[*d*]imidazol-4-yl)(phenyl)methyl)acetamide (1).** An oven-dried 25 mL Schlenk tube was charged with **6** (147 mg, 0.390 mmol), *N*-(phenyl(4,4,5,5-tetramethyl-1,3,2-dioxaborolan-2-yl)methyl)acetamide[6] (269 mg, 0.978 mmol), $Pd_2(dba)_3$ (19.5 mg, 21.3 μmol), $P(tBu)_3{\cdot}HBF_4$ (26.8 mg, 92.3 μmol), KF (113 mg, 1.94 mmol), 1,4-dioxane (2 mL), and H_2O (23 μL). Freeze-pump-thaw cycles (× 2) were applied to remove oxygen. The reaction mixture was heated at reflux for 24 h, cooled to r.t., poured into water (100 mL), and extracted into EtOAc (100 mL × 3). The combined extracts were dried over anhyd $MgSO_4$, filtered, and concentrated under reduced pressure. Flash column chromatography on SiO_2 (hexane:EtOAc = 9:1 to 1:9, v/v) furnished **1** containing a small amount of impurity. The resulting solid was recrystallized from EtOAc to provide analytically pure **1** as a white solid (29.1 mg, 65.3 μmol, yield = 17%). ^{1}H NMR (500 MHz, $CDCl_3$, 298 K): δ 13.28 (s, 1H), 12.11 (s, 1H), 10.15 (s, 1H), 7.76 (d, J = 7.7 Hz, 1H), 7.48 (d, J = 7.5 Hz, 1H), 7.39 (d, J = 7.5 Hz, 2H), 7.36–7.27 (m, 3H), 7.25–7.23 (m, 1H), 6.86 (d, J = 7.0 Hz, 1H), 6.79 (d, J = 8.3 Hz, 1H), 6.76–6.67 (m, 2H), 5.52 (s, 2H), 3.65 (s, 3H), 2.12 (s, 3H). ^{13}C NMR (150 MHz, $CDCl_3$, 298 K): δ 192.3, 169.7, 161.1, 156.0, 152.5, 140.8, 138.9, 138.3, 132.8, 131.2, 129.2, 128.2, 127.4, 121.7, 120.9, 112.1, 104.5, 102.6, 95.6, 57.5, 56.4, 23.8, 1.4. FT-IR (ATR, cm^{-1}): 3431, 3243, 3036, 2931, 2843, 1670, 1646, 1613, 1588, 1526, 1490, 1473, 1452, 1418, 1402, 1358, 1263, 1245, 1203, 1179, 1162, 1120, 1082, 1041, 964, 941, 918, 840, 828, 797, 789, 775, 759, 745, 698, 660. HRMS (ESI) calcd for $C_{25}H_{23}N_3O_5$ $[M + H]^+$ 446.1711, found 446.1713.

X-ray Crystallographic Studies on 4. Single crystals of **4** were prepared by slow evaporation of an EtOAc solution of this material. A colorless crystal (approximate dimensions 0.038 × 0.055 × 0.733 mm^3) was placed onto a nylon loop with Paratone-N oil, and mounted on a XtaLAB AFC12 (RINC): Kappa dual home/near diffractometer. The data collection was carried out using Cu Kα radiation, and the crystal was kept at T = 93 K. A total of 16079 reflections were measured (10.172° ≤ 2θ ≤ 158.25°). The structure was solved with SHELXT[11] using intrinsic phasing methods, and refined with SHELXL[12] refinement package of OLEX2.[13] A total 2987 unique reflections were used in all calculations. The final $R1$ was 0.0830 ($I \geq 2\sigma(I)$) and $wR2$ was 0.2396 (all data).

[11] G. M. Sheldrick, *Acta Cryst.,* 2015, **A71**, 3–8.
[12] G. M. Sheldrick, *Acta Cryst.,* 2015, **C71**, 3–8.
[13] O. V. Dolomanov, L. J. Bourhis, R. J. Gildea, J. A. K. Howard and H. Puschmann, *J. Appl. Cryst.,* 2009, **42**, 339–341.

X-ray Crystallographic Studies on 6. Single crystals of **6** were prepared by slow evaporation of a $CHCl_3$ solution of this material. A pale yellow crystal (approximate dimensions 0.121 × 0.183 × 0.832 mm^3) was placed onto a nylon loop with Paratone-N oil, and mounted on a XtaLAB AFC12 (RINC): Kappa dual home/near diffractometer. The data collection was carried out using Cu Kα radiation, and the crystal was kept at $T = 93$ K. A total of 32612 reflections were measured ($7.428° \leq 2\theta \leq 158.47°$). The structure was solved with SHELXT[11] using intrinsic phasing methods, and refined with SHELXL[12] refinement package of OLEX2.[13] A total 8119 unique reflections were used in all calculations. The final $R1$ was 0.0740 ($I \geq 2\sigma(I)$) and $wR2$ was 0.2013 (all data).

X-ray Crystallographic Studies on 1. Single crystals of **1** were prepared by slow diffusion of pentane into a $CHCl_3$ solution of this material. A colorless crystal (approximate dimensions 0.04 × 0.12 × 0.13 mm^3) was placed onto a nylon loop with Paratone-N oil, and mounted on a PHOTON 100 CMOS diffractometer. The data collection was carried out using Cu Kα radiation, and the crystal was kept at $T = 223.15$ K. A total of 62856 reflections were measured ($8.154° \leq 2\theta \leq 155.552°$). The structure was solved with SHELXT[11] using intrinsic phasing methods, and refined with SHELXL[12] refinement package of OLEX2.[13] A total 4599 unique reflections were used in all calculations. The final $R1$ was 0.0508 ($I \geq 2\sigma(I)$) and $wR2$ was 0.1146 (all data).

Table S1. Summary of X-ray Crystallographic Data.

	4	**6**	**1**
Chemical formula	$C_{16}H_{14}N_2O_4$	$C_{34}H_{28}Br_2Cl_6N_4O_8$	$C_{25}H_{23}N_3O_5$
Formula weight	298.29	950.64	445.46
Crystal system	monoclinic	monoclinic	monoclinic
Space group	$I2/a$	$P2_1/c$	$P2_1/c$
Color of crystal	colorless	light yellow	colorless
a (Å)	17.4514(4)	25.8801(5)	11.2876(6)
b (Å)	4.6477(1)	6.9453(1)	21.068(1)
c (Å)	35.6080(8)	23.8077(4)	9.7510(5)
α (°)			
β (°)	102.334(2)	116.121(2)	106.139(3)
γ (°)			
Volume (Å^3)	2821.5(1)	3842.3(1)	2227.5(2)
Z	7	17	4
R_{int}	0.1365	0.0839	0.0899
Final R indices [$I \geq 2\sigma(I)$]	$R1 = 0.0830$, $wR2 = 0.2263$	$R1 = 0.0740$, $wR2 = 0.2007$	$R1 = 0.0508$, $wR2 = 0.0990$
Final R indices [all data]	$R1 = 0.0922$, $wR2 = 0.2396$	$R1 = 0.0755$, $wR2 = 0.2013$	$R1 = 0.0813$, $wR2 = 0.1146$
Goodness-of-fit on F^2	1.078	1.110	1.026

Density Functional Theory (DFT) Calculations. All density functional theory (DFT) calculations were conducted using Gaussian '09 Revision E.01 software.[14] All geometry optimizations and vibrational frequency calculations were carried out with B3LYP hybrid functional with Gimme's D3 dispersion correction (B3LYP-D3) and 6-31G(d,p) basis set.

Table S2. Cartesian Coordinates of the Optimized Geometry of **1**.

Atom	x	y	z
C	-0.491756	1.069277	-0.334097
C	-0.583223	3.837741	-0.14069
C	-1.747719	1.695939	-0.358467
C	0.695445	1.824657	-0.221711
C	0.679307	3.227339	-0.116902
C	-1.763408	3.091477	-0.261275
N	1.717748	0.913392	-0.235089
C	1.158246	-0.337389	-0.343659
N	-0.173016	-0.271076	-0.411409
C	1.874349	-1.607391	-0.300674
C	3.197913	-4.077188	-0.042758
C	3.250393	-1.737347	-0.586617
C	1.155693	-2.783069	0.071438
C	1.83817	-4.000112	0.218524
C	3.912669	-2.951637	-0.465903
O	-0.163905	-2.782496	0.312101
O	3.917824	-0.635145	-1.103435
C	4.970673	-0.093748	-0.354115
O	4.402853	0.719155	0.651921
C	5.286042	1.702356	1.181216
C	1.91011	4.00344	0.021991
O	3.031477	3.514666	0.075032
C	-3.023109	0.873969	-0.452093
N	-2.988593	0.057112	-1.659338
C	-4.073018	-0.524645	-2.276701
O	-3.920608	-1.379547	-3.138192
C	-5.446651	-0.032566	-1.849463
C	-3.234226	0.077858	0.845266
C	-3.561542	-1.305509	3.264238
C	-3.124806	-1.314153	0.883585
C	-3.517944	0.771558	2.0282
C	-3.683638	0.086166	3.23008
C	-3.281584	-2.001919	2.088971

Atom	x	y	z
H	-3.854944	1.579061	-0.548125
H	-0.641728	4.920308	-0.064296
H	-2.717487	3.609763	-0.280876
H	2.703202	1.118774	-0.066189
H	3.709641	-5.029787	0.055164
H	1.264158	-4.868335	0.521198
H	4.96056	-3.018422	-0.735507
H	-0.51829	-1.877648	0.106331
H	5.567776	0.507441	-1.052757
H	5.596252	-0.878111	0.09939
H	4.701963	2.301272	1.878914
H	6.130099	1.235816	1.707776
H	5.664286	2.363244	0.390687
H	1.769054	5.10408	0.0815
H	-2.105719	-0.388416	-1.88164
H	-5.561582	1.039533	-2.043233
H	-5.608765	-0.200151	-0.779676
H	-6.192555	-0.582237	-2.422035
H	-3.684176	-1.840923	4.201014
H	-2.91449	-1.865285	-0.026468
H	-3.596878	1.855975	2.006736
H	-3.905409	0.63678	4.139795
H	-3.177398	-3.082408	2.103456

[14] M. J. Frisch, G. W. Trucks, H. B. Schlegel, G. E. Scuseria, M. A. Robb, J. R. Cheeseman, G. Scalmani, V. Boarone, B. Mennucci, G. A. Petersson et al. Gaussian '09 , revision E.01; Gaussian, Inc.: Wallingford CT, 2009.

Table S3. Vibrational Frequences (cm^{-1}) of the Optimized Structure of **1**.

18.4873	20.7007	38.3784	45.6317	47.8926	51.1334
55.8766	65.7067	69.5381	80.7537	96.2855	105.976
114.592	132.996	157.726	179.394	182.023	186.074
201.44	209.134	214.684	224.873	230.748	247.897
261.477	275.321	303.528	330.255	354.233	365.077
371.556	401.266	415.709	421.497	448.214	494.788
501.616	505.154	525.378	533.757	551.864	557.298
571.604	575.79	588.635	599.269	616.451	632.357
646.389	659.269	662.641	669.228	685.877	712.663
716.156	724.128	746.173	764.466	781.318	787.724
792.462	799.464	802.119	813.639	843.211	854.481
862.977	871.148	878.075	935.097	939.798	970.443
971.205	980.497	985.167	1001.41	1004.71	1016.79
1023.53	1030.72	1056.83	1057.42	1071.72	1090.8
1110.35	1111.63	1123.5	1132.03	1145.53	1154.88
1163.41	1192.92	1196.05	1198.34	1204.78	1206.69
1219.39	1229.25	1251.13	1256.51	1266.49	1293.84
1304.56	1312.61	1317.47	1341.88	1351.45	1363.08
1364.76	1366.58	1368.05	1401.87	1414.47	1423.6
1437.85	1439.71	1449.43	1469.27	1487.65	1490.77
1491.69	1494.74	1499.65	1505.01	1509.92	1513.04
1534.6	1537.94	1540.3	1549.24	1572.6	1631.28
1642.4	1647.63	1655.17	1660.68	1677.36	1763.04
1795	2916.48	2992.27	3009.91	3048.16	3055.41
3065.7	3074.22	3114.67	3167.35	3168.6	3176.21
3178.02	3182.35	3190.93	3193.42	3194.66	3203.68
3213.48	3214.85	3222.6	3259.85	3452.67	3589.65

Table S4. Cartesian Coordinates of the Optimized Geometry of the Cyanohydrin Adduct of **1**.

Atom	x	y	z
C	0.528335	-0.75749	-0.288165
C	0.463057	-3.518507	0.078703
C	1.723322	-1.479887	-0.458504
C	-0.684157	-1.42177	0.046471
C	-0.723443	-2.810558	0.245592
C	1.658696	-2.862778	-0.27472
N	-1.693106	-0.500164	0.179593
C	-1.082994	0.675878	-0.086941
C	-1.707098	2.005717	-0.000627
C	-2.82381	4.581084	0.361017
C	-3.099517	2.221651	-0.075056
C	-0.87626	3.151821	0.189619
C	-1.444221	4.417211	0.394417
C	-3.655241	3.490267	0.108929
O	0.4687	3.071642	0.185255
O	-3.942706	1.188335	-0.418202
C	-2.039684	-3.458405	0.640598
O	-2.815521	-2.652214	1.503942
C	-4.752223	0.663146	0.638615
O	-5.747833	-0.127804	0.094425
C	-5.256918	-1.357295	-0.454556
C	3.054961	-0.801391	-0.744566
C	-2.821476	-3.826	-0.579294
N	2.881391	0.30152	-1.690094
C	3.857464	0.896858	-2.436072
O	3.635519	1.890538	-3.121591
C	5.237415	0.248236	-2.400492
C	3.735011	-0.373127	0.560898
C	4.983845	0.36082	2.970161
C	3.259947	0.716336	1.304023
C	4.837831	-1.086967	1.041338
C	5.461208	-0.72578	2.238162
C	3.88045	1.077822	2.498056

Atom	x	y	z
H	3.702455	-1.550884	-1.213524
N	-3.443608	-4.124269	-1.514177
H	0.470115	-4.596696	0.221687
H	2.566028	-3.451471	-0.389199
H	-3.254188	5.569217	0.502912
H	-0.77108	5.252997	0.553528
H	-4.730205	3.603651	0.014797
H	-1.83913	-4.402312	1.165145
H	-2.697961	-1.727448	1.176519
H	-5.249739	1.482822	1.174384
H	-4.100324	0.103806	1.328716
H	-6.101461	-1.835583	-0.955363
H	-4.454651	-1.180126	-1.176008
H	-4.879745	-2.016559	0.335337
H	1.985887	0.781542	-1.672907
H	5.202189	-0.775411	-2.79073
H	5.629313	0.199017	-1.37992
H	5.902018	0.846266	-3.023624
H	5.466052	0.648438	3.900596
H	2.395834	1.269629	0.955887
H	5.212625	-1.934497	0.471397
H	6.319469	-1.290632	2.593069
H	3.497744	1.923193	3.063055
N	0.250271	0.583402	-0.377426
H	0.691845	2.13229	-0.097297

Table S5. Vibrational Frequences (cm^{-1}) of the Optimized Structure of the Cyanohydrin Adduct of **1**.

17.881	25.7289	31.9568	38.4493	48.5499	55.7138
60.8485	65.6882	75.8295	83.4569	85.2509	89.1068
104.399	112.829	144.67	152.252	163.667	177.635
188.483	194.907	198.789	207.831	222.477	239.289
245.892	254.856	264.248	279.814	309.589	329.756
340.279	351.675	380.743	395.812	414.151	420.06
435.203	451.246	482.741	506.385	518.693	530.391
536.692	552.586	566.411	575.497	589.24	604.875
610.917	616.002	628.822	637.16	645.875	666.934
673.527	680.752	707.093	715.205	717.493	739.607
747.732	762.756	776.452	786.433	788.246	795.697
811.12	845.078	845.51	859.41	860.554	864.678
889.18	898.559	920.639	928.438	945.544	960.905
968.869	983.59	993.333	998.228	1017.37	1029.61
1054.27	1055.36	1058.78	1062.08	1076.01	1088.87
1106.96	1109.35	1119.34	1144.99	1157.48	1185.09
1186.12	1189.17	1192.15	1197.24	1208.9	1217.21
1225.69	1236.37	1262.22	1264.87	1301.11	1307.62
1309.39	1312.74	1327.14	1331.21	1337.53	1346.23
1360.5	1365.43	1371.23	1385.52	1388.77	1414.93
1418.93	1443.01	1457.79	1489	1490.26	1494.52
1501.21	1503.54	1505.91	1506.38	1508.09	1531.49
1532.91	1536.28	1542.82	1553.62	1574.18	1633.43
1637.92	1639.65	1641.51	1658.08	1675.42	1782.33
2342.48	2984.5	3005.64	3030.49	3041.98	3042.5
3044.57	3047.64	3114.19	3122.43	3143.34	3153.74
3156.67	3167.68	3168.55	3169.64	3173.25	3182.22
3194.87	3199.74	3206.96	3233.25	3390.44	3537.61

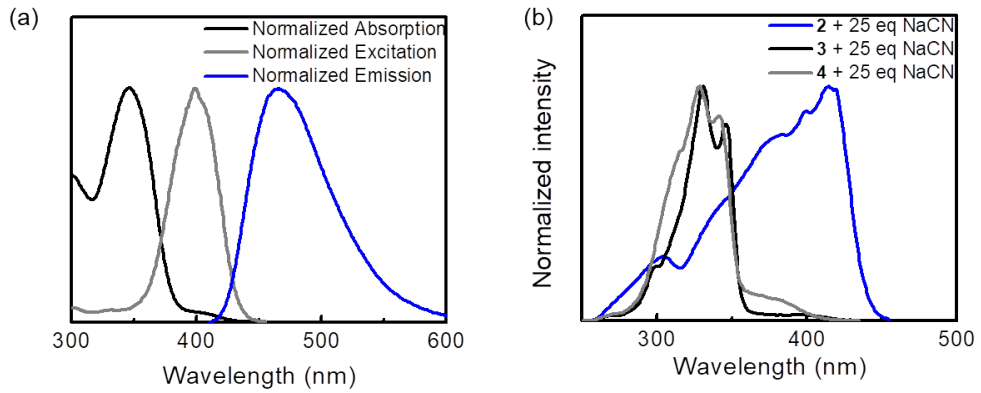

Fig. S1. (a) Normalized absorption (black line), excitation (λ_{em} = 465 nm, gray line), and emission (λ_{exc} = 400 nm, blue line) spectra of **2** (0.100 mM) treated with Et_3N (25 equiv) in DMSO at T = 298 K. (b) Normalized excitation (λ_{em} = 465 nm for **2**; λ_{em} = 445 nm for **3** and **4**) spectra of **2** (blue line), **3** (black line), and **4** (gray line) treated with NaCN (25 equiv) in DMSO at T = 298 K.

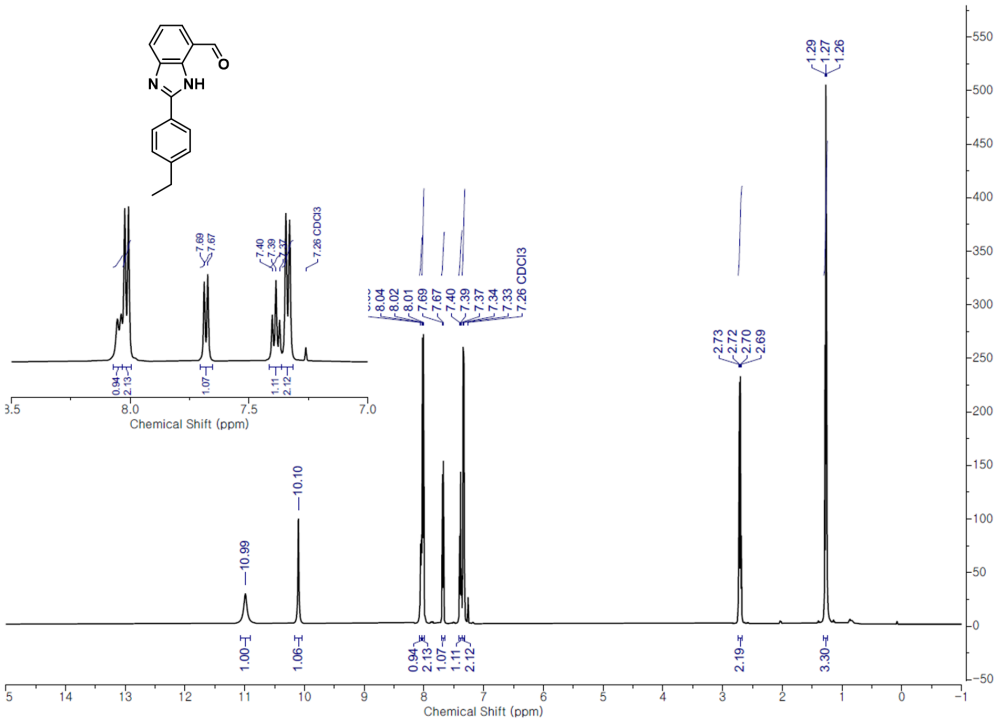

Fig. S2. ^{1}H NMR (500 MHz) spectrum of **2** in $CDCl_3$ (T = 298 K).

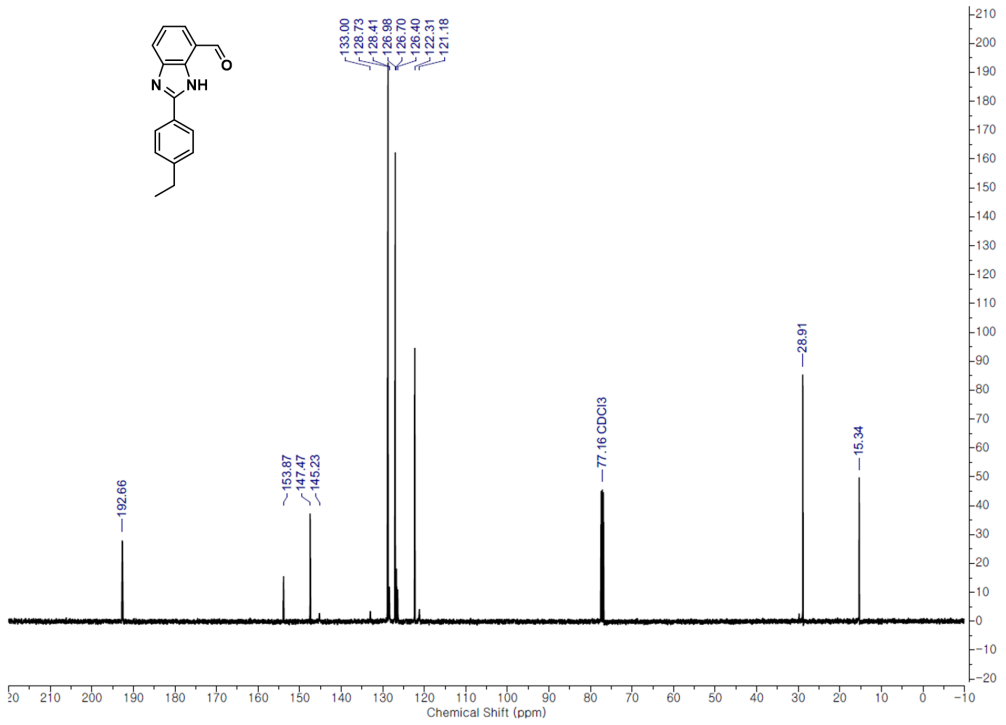

Fig. S3. ^{13}C NMR (125 MHz) spectrum of **2** in $CDCl_3$ (T = 298 K).

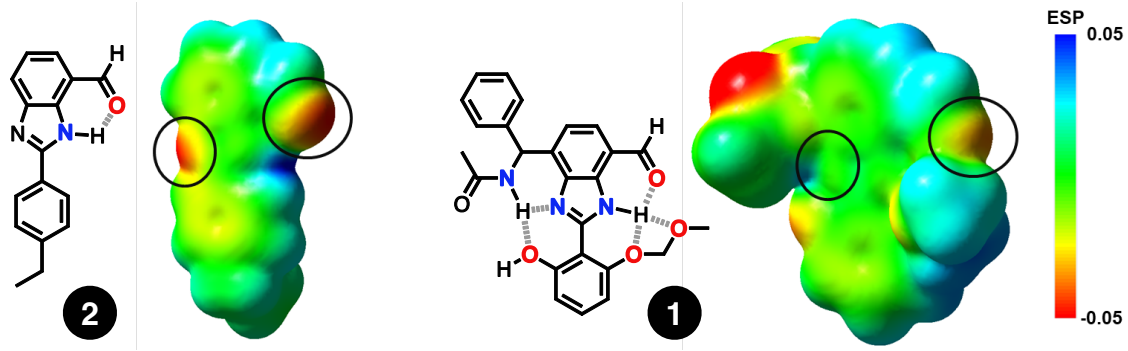

Fig. S4. Molecular electrostatic potential (MEP) maps of **1** and **2** calculated at the B3LYP-D3/6-31g(d,p) level. The circled regions (in black) denote the aldehyde oxygen and benzimidazole sp^2-nitrogen atoms of each molecule.

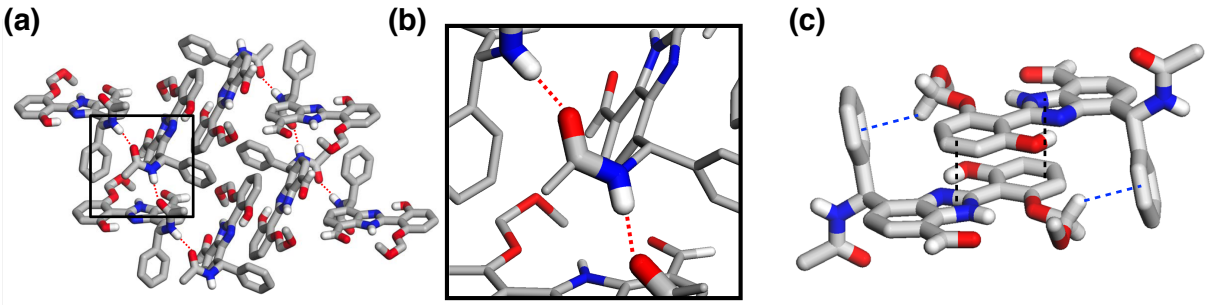

Fig. S5. Capped-stick representation of the X-ray structure of **1** showing (a) intermolecular hydrogen-bonding network (red dotted lines) of amide groups belonging to adjacent molecules in the crystal lattice, (b) close-up view of the intermolecular N–H$\cdots$O contacts (red dotted lines), and (c) C–H$\cdots\pi$ (blue dashed lines) and $\pi\cdots\pi$ (black dashed lines) interactions between "dimeric **1**" in the solid-state.

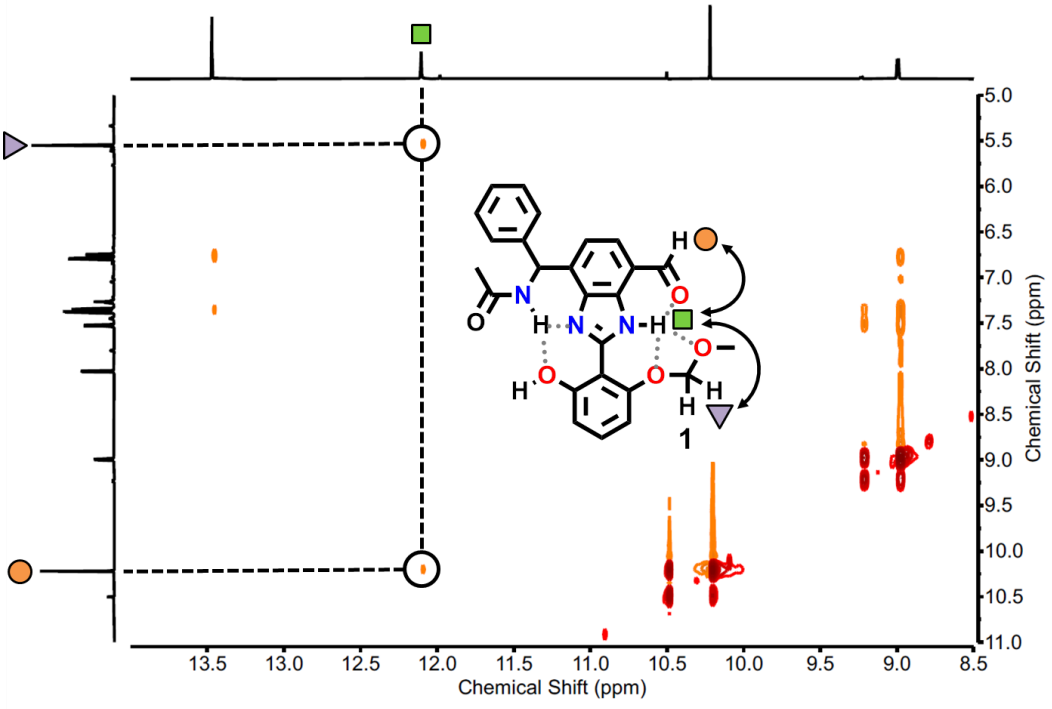

Fig. S6. Partial 2D ROESY contour plot of **1** (4.0 mM) in DMSO-d_6 at T = 298 K. The corresponding 1D NMR spectrum is shown along the ordinate.

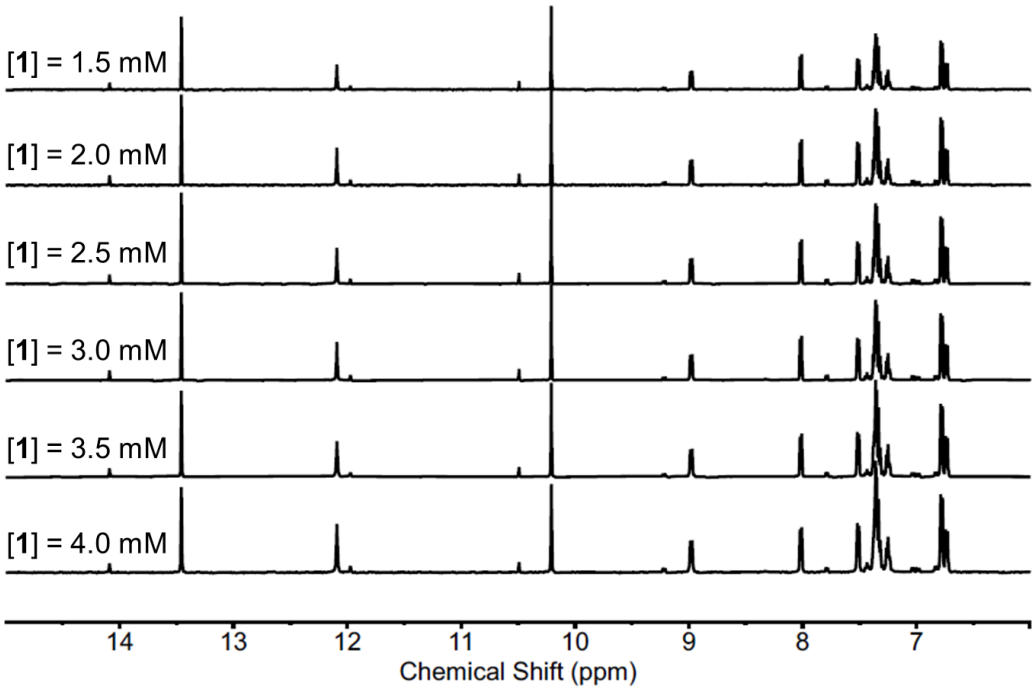

Fig. S7. Concentration-dependent ^{1}H NMR spectra of **1** in DMSO-d_6 at $T = 25$ °C.

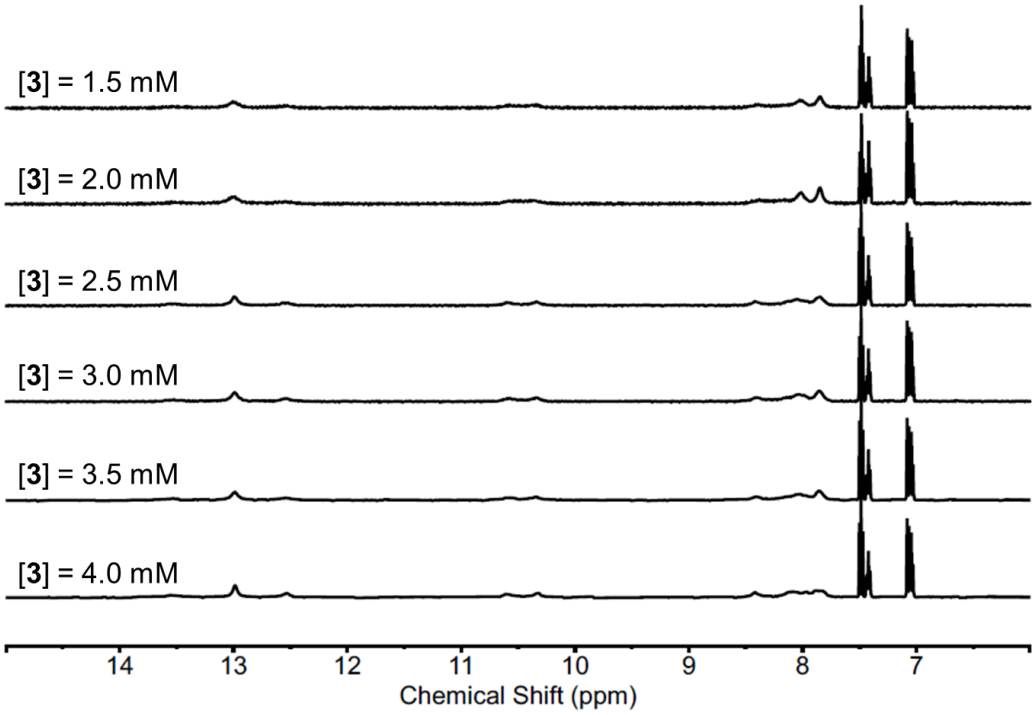

Fig. S8. Concentration-dependent ^{1}H NMR spectra of **3** in DMSO-d_6 at $T = 25$ °C.

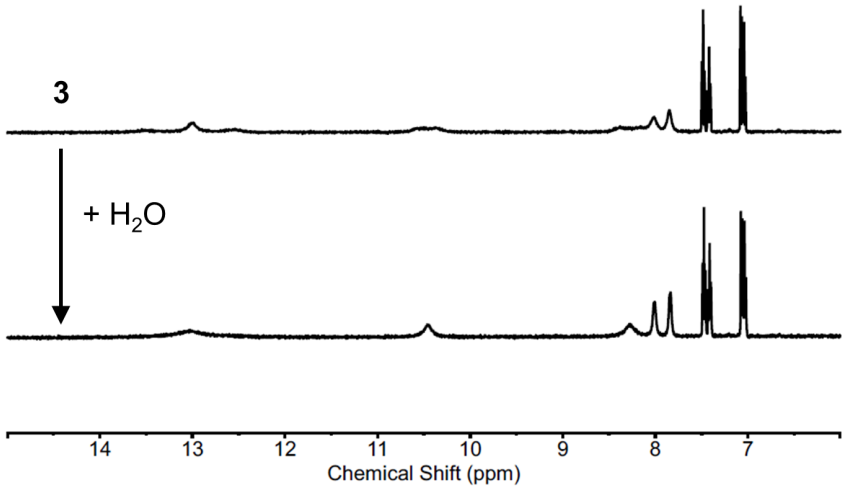

Fig. S9. ^{1}H NMR spectral changes of **3** in DMSO-d_6 (2.0 mM, 500 μL) prior to (top) and after (bottom) treatment with H_2O (2 μL).

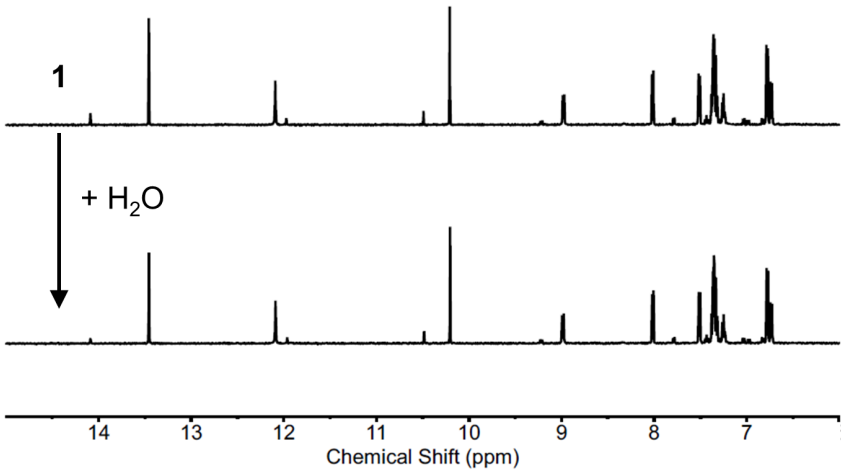

Fig. S10. ^{1}H NMR spectral changes of **1** in DMSO-d_6 (2.0 mM, 500 μL) prior to (top) and after (bottom) treatment with H_2O (2 μL).

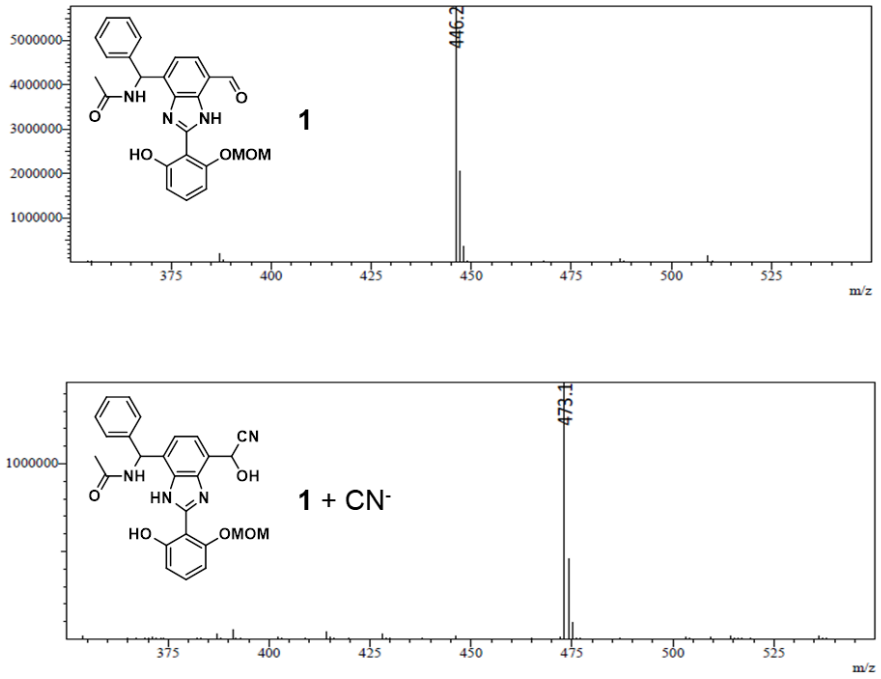

Fig. S11. HPLC-MS analysis of **1** (top) and **1** treated with NaCN (25 equiv, bottom) in DMSO. MS (ESI) calcd for $C_{25}H_{24}N_3O_5$ [**1** + H]$^+$, 446.1710; found, 446.20. Calcd for $C_{26}H_{25}N_4O_5$ [**1** + CN + 2H]$^+$, 473.1819; found, 473.15.

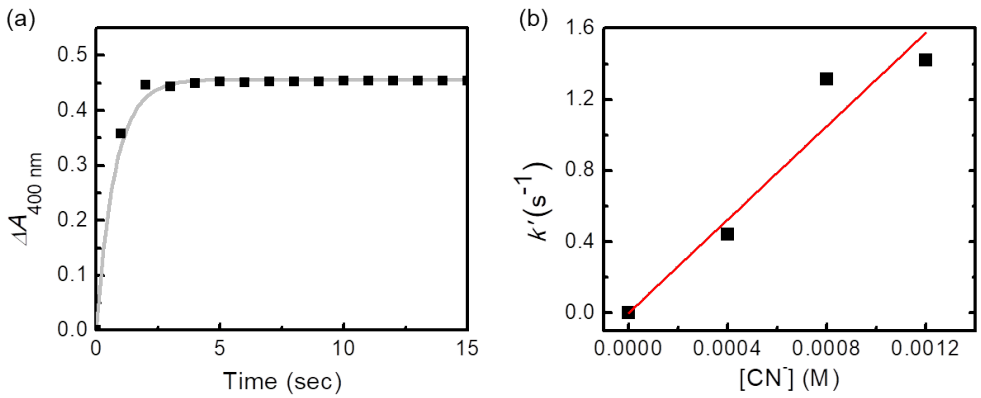

Fig. S12. (a) Time-dependent changes in the UV–vis absorption at $\lambda = 400$ nm upon the reaction of **1** (40.0 μM) with NaCN (20 equiv) in DMSO–MeCN (1:1, v:v) at $T = 288$ K. The gray curve overlaid on the experimental data points is a theoretical fit using $k' = 1.3$ s^{-1}. (b) Plot of k' ($= k_2[\mathrm{CN}^-]_0$) vs $[\mathrm{CN}^-]_0$ to estimate the second-order rate constant $k_2 = 1.3 \times 10^3$ M^{-1} s^{-1}.

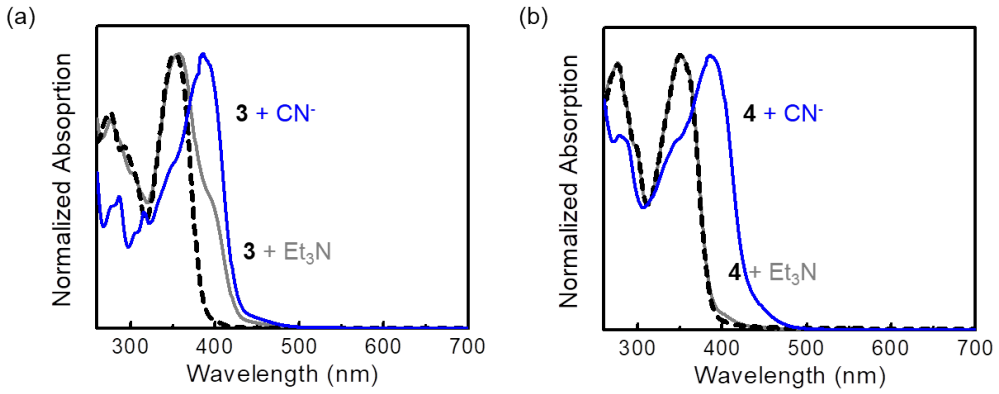

Fig. S13. (a) Absorption spectra of **3** (0.100 mM) prior to (black dashed line), and after treatment with NaCN (25 equiv, blue line) or Et_3N (25 equiv, gray line) in DMSO. (b) Absorption spectra of **4** (0.100 mM) prior to (black dashed line), and after treatment with NaCN (25 equiv, blue line) or Et_3N (25 equiv, gray line) in DMSO. T = 298 K.

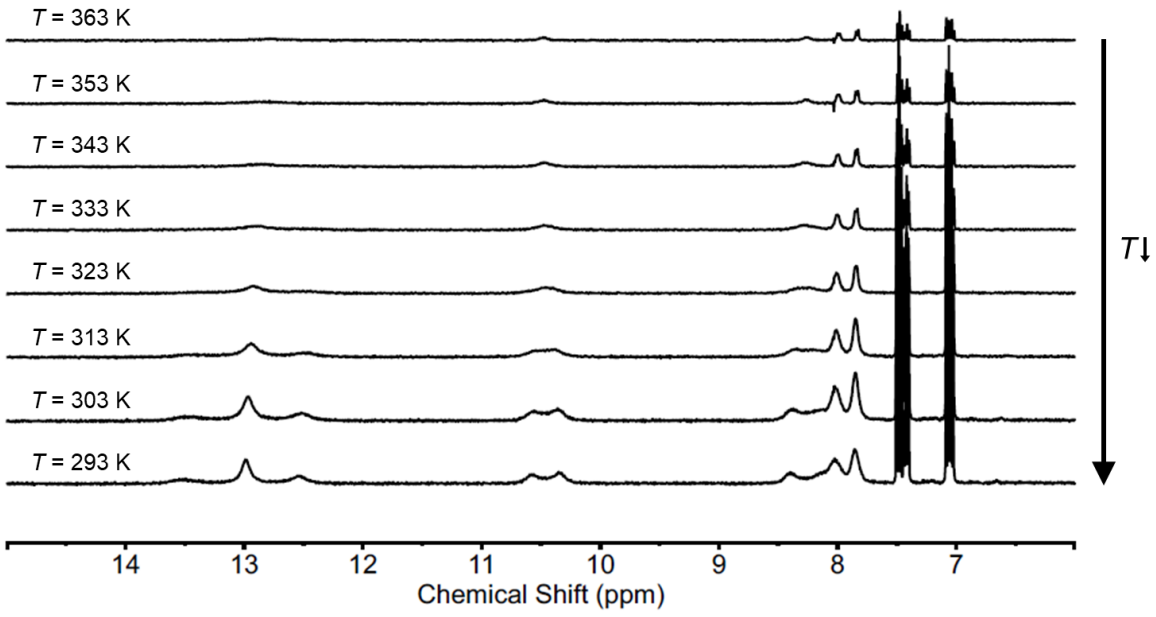

Fig. S14. Variable-temperature ^{1}H NMR spectra of **3** (4.0 mM) in DMSO-d_6 at T = 293–363 K.

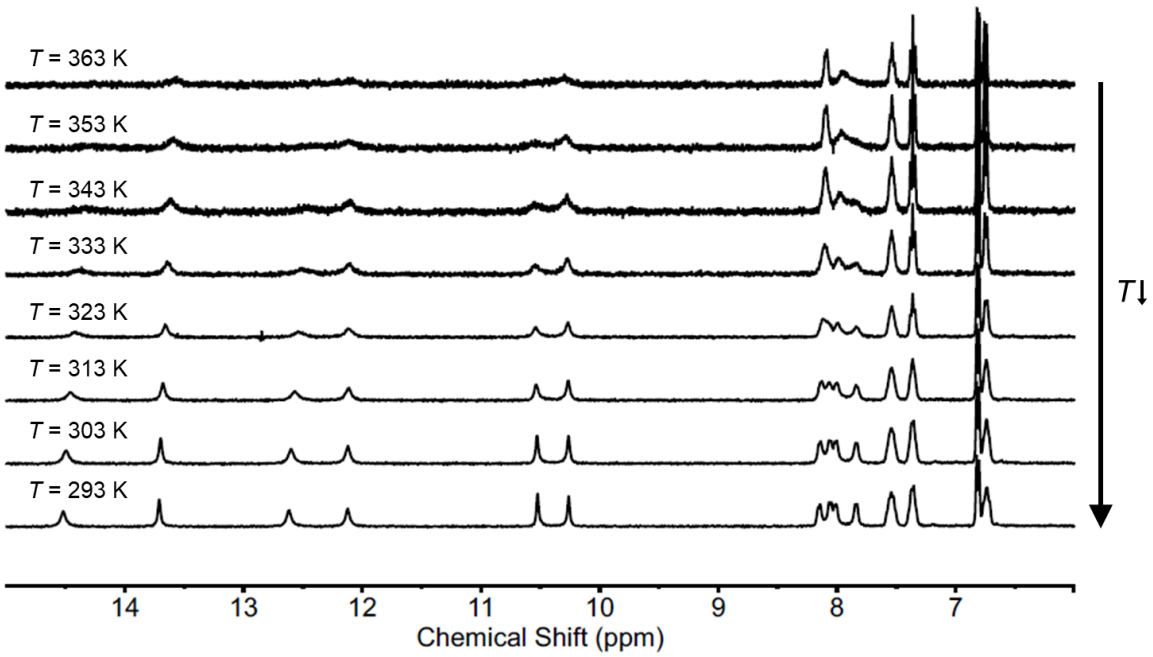

Fig. S15. Variable-temperature ^{1}H NMR spectra of **4** (4.0 mM) in DMSO-d_6 at T = 293–363 K.

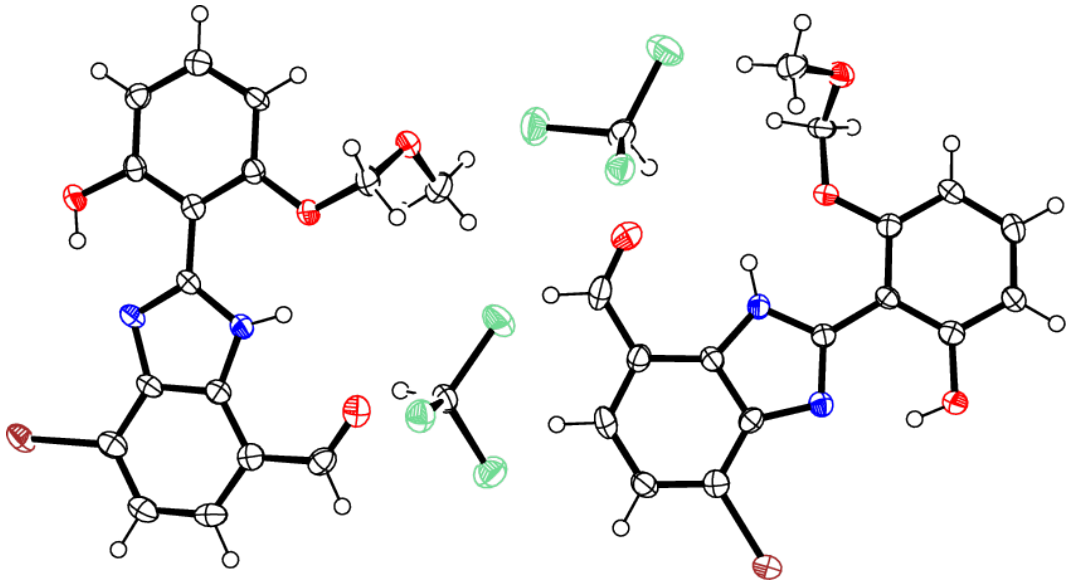

Fig. S16. X-ray structure of **6** as an ORTEP diagram with thermal ellipsoids at the 50% probability level.

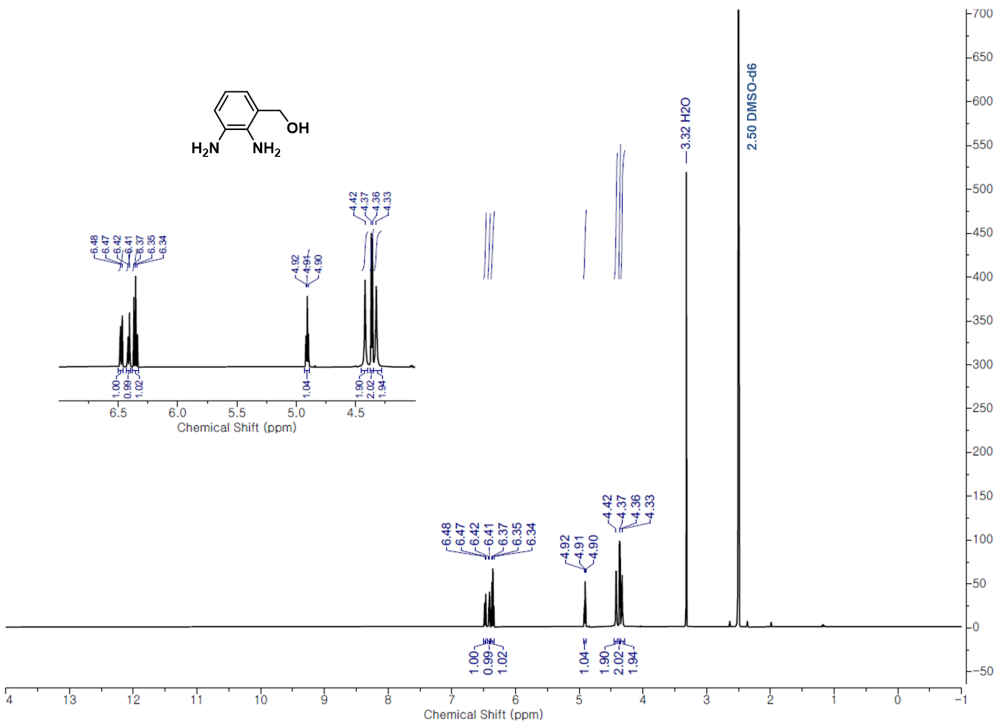

Fig. S17. ^{1}H NMR (500 MHz) spectrum of **5** in DMSO-d_6 (T = 298 K).

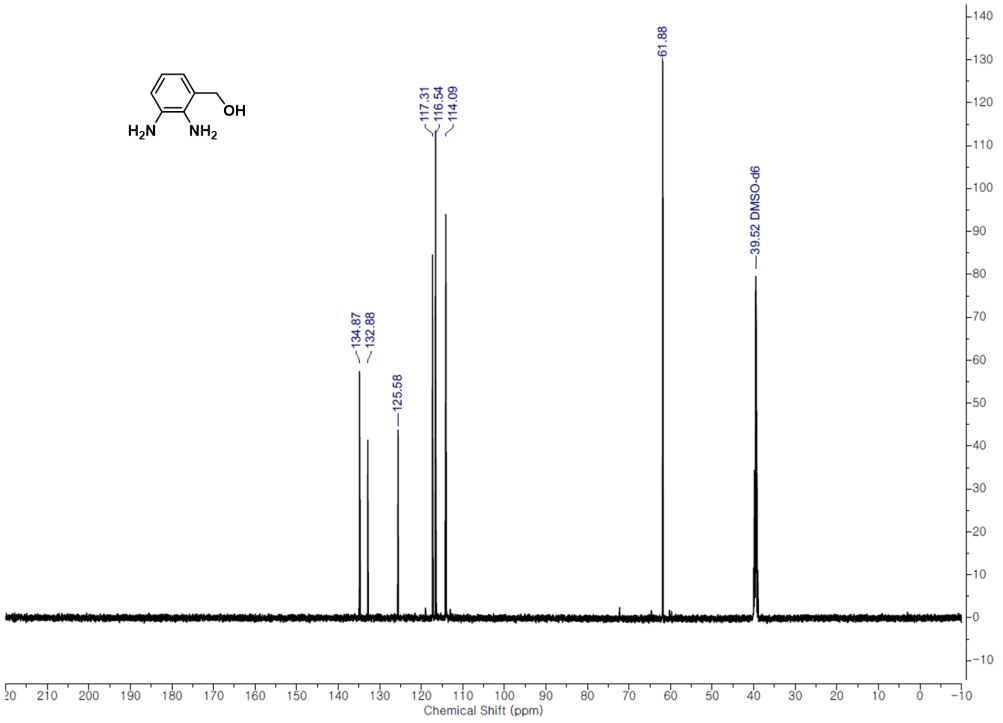

Fig. S18. ^{13}C NMR (125 MHz) spectrum of **5** in DMSO-d_6 (T = 298 K).

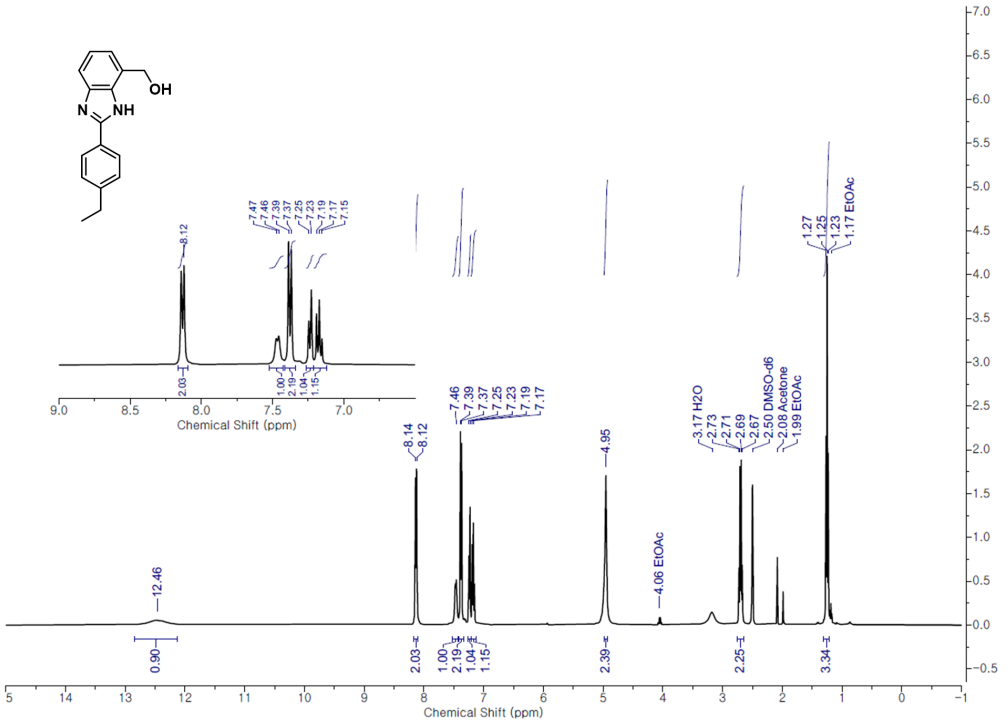

Fig. S19. ^{1}H NMR (400 MHz) spectrum of **7** in DMSO-d_6 (T = 343 K).

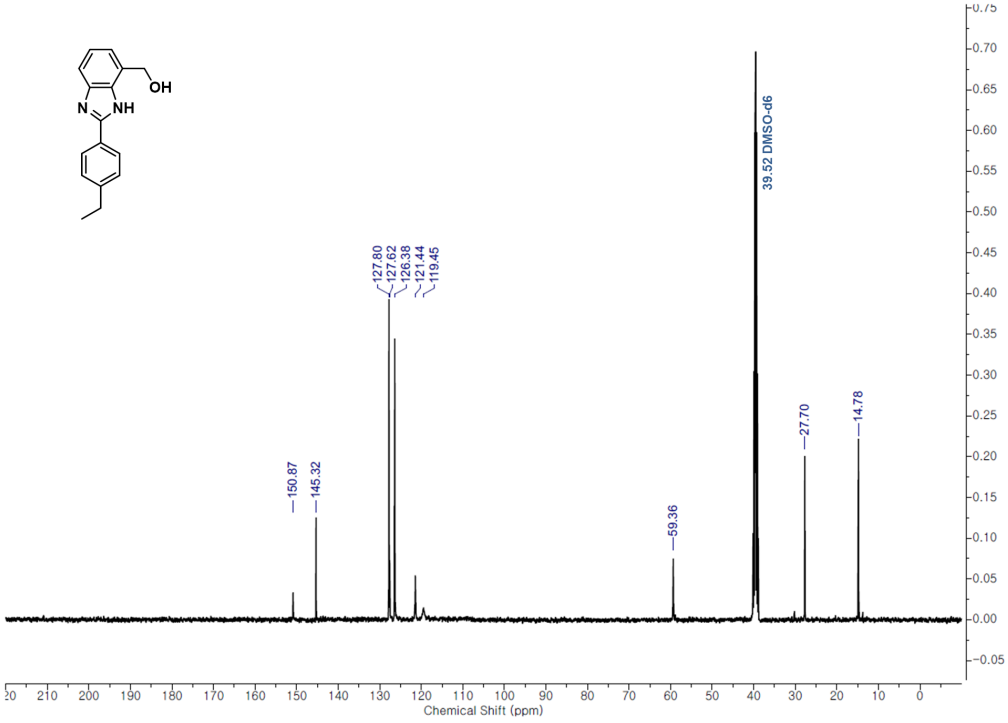

Fig. S20. ^{13}C NMR (100 MHz) spectrum of **7** in DMSO-d_6 (T = 343 K).

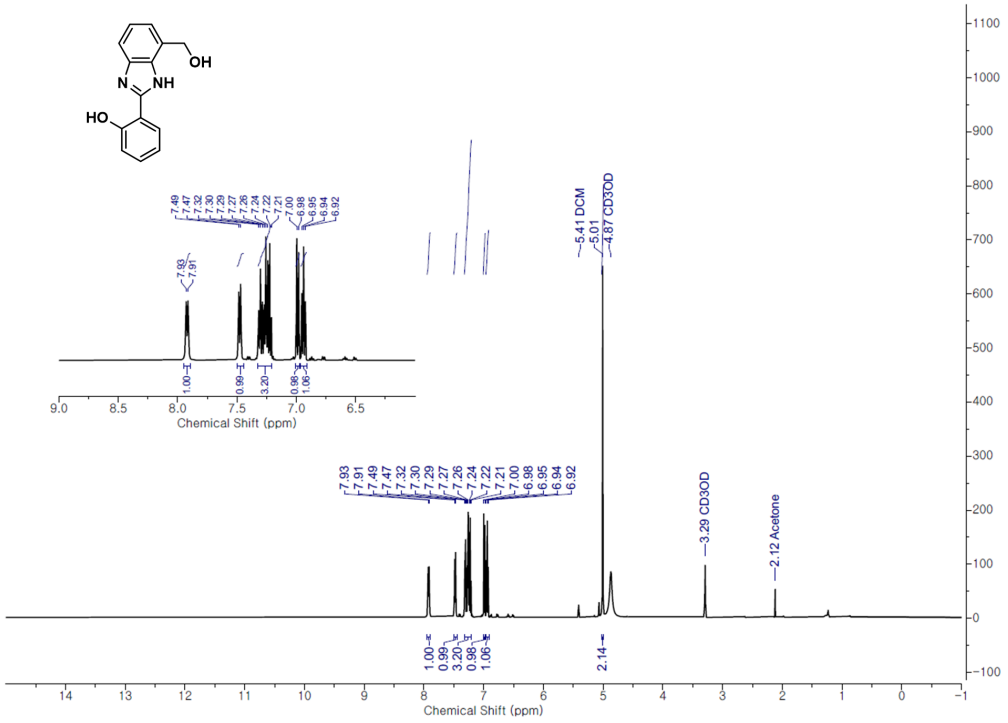

Fig. S21. ^{1}H NMR (500 MHz) spectrum of **8** in CD_3OD (T = 298 K).

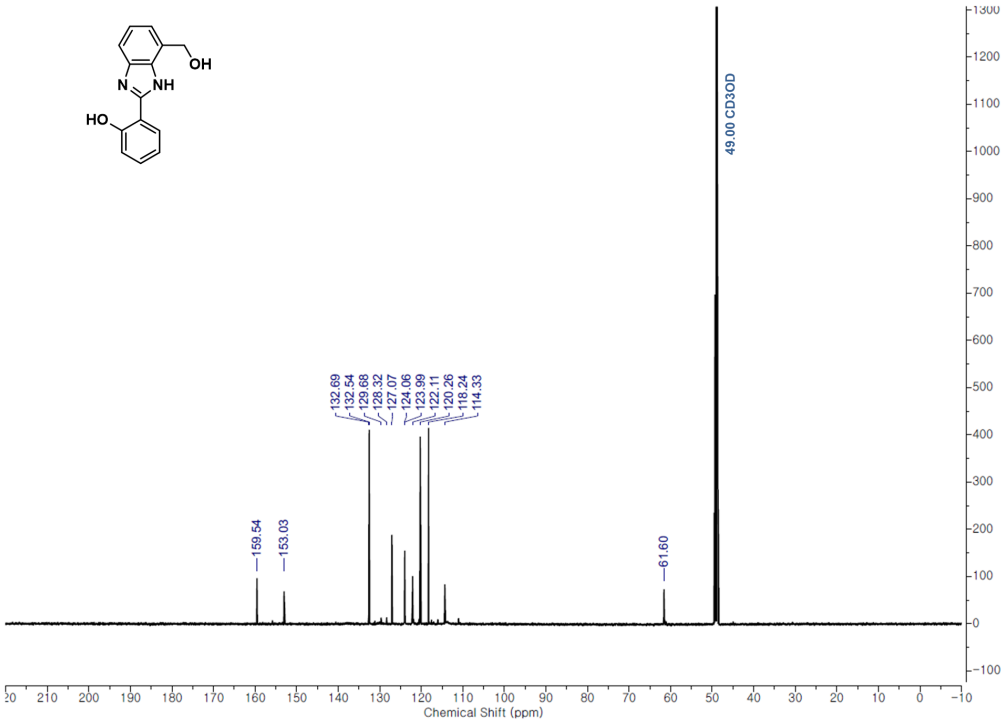

Fig. S22. ^{13}C NMR (125 MHz) spectrum of **8** in CD_3OD (T = 298 K).

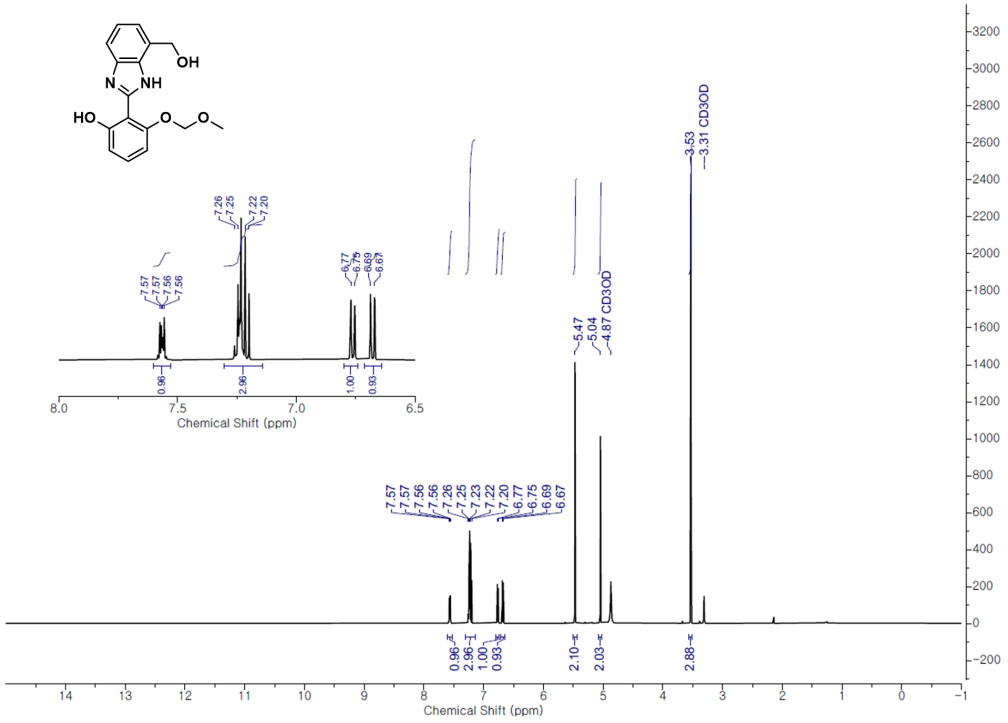

Fig. S23. ^{1}H NMR (500 MHz) spectrum of **9** in CD_3OD (T = 298 K).

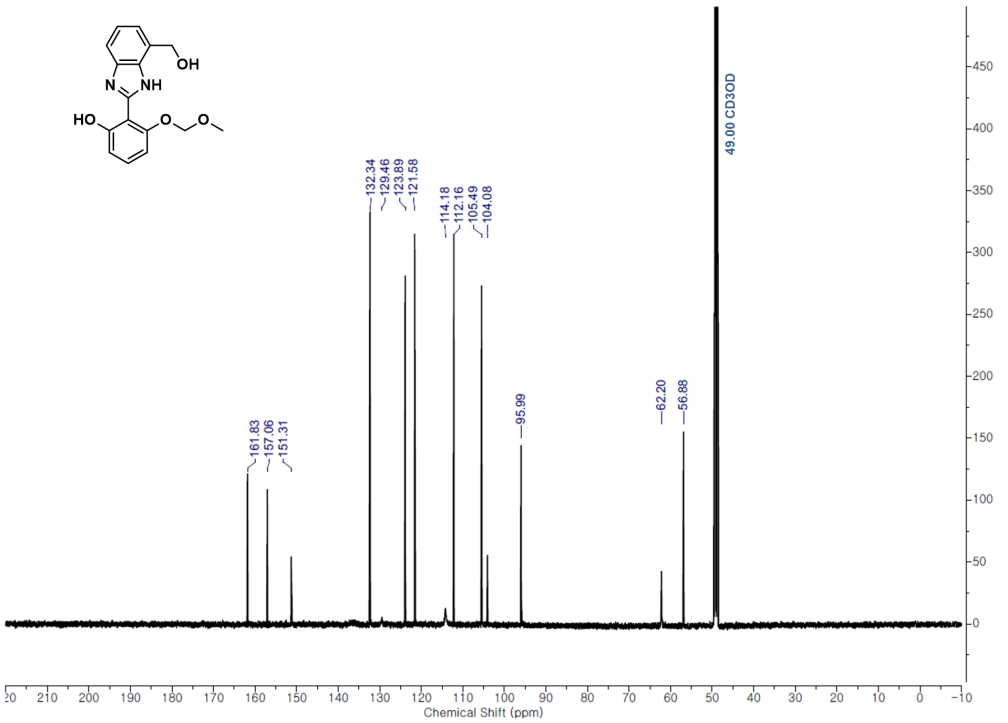

Fig. S24. ^{13}C NMR (125 MHz) spectrum of **9** in CD_3OD (T = 298 K).

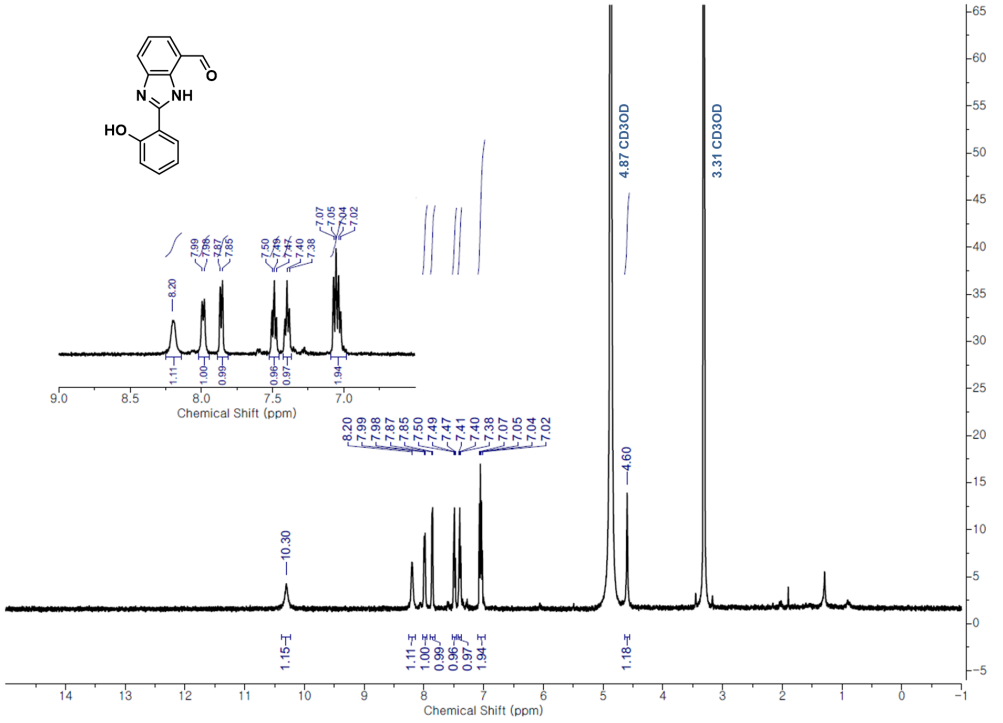

Fig. S25. ^{1}H NMR (500 MHz) spectrum of **3** in CD_3OD (T = 298 K).

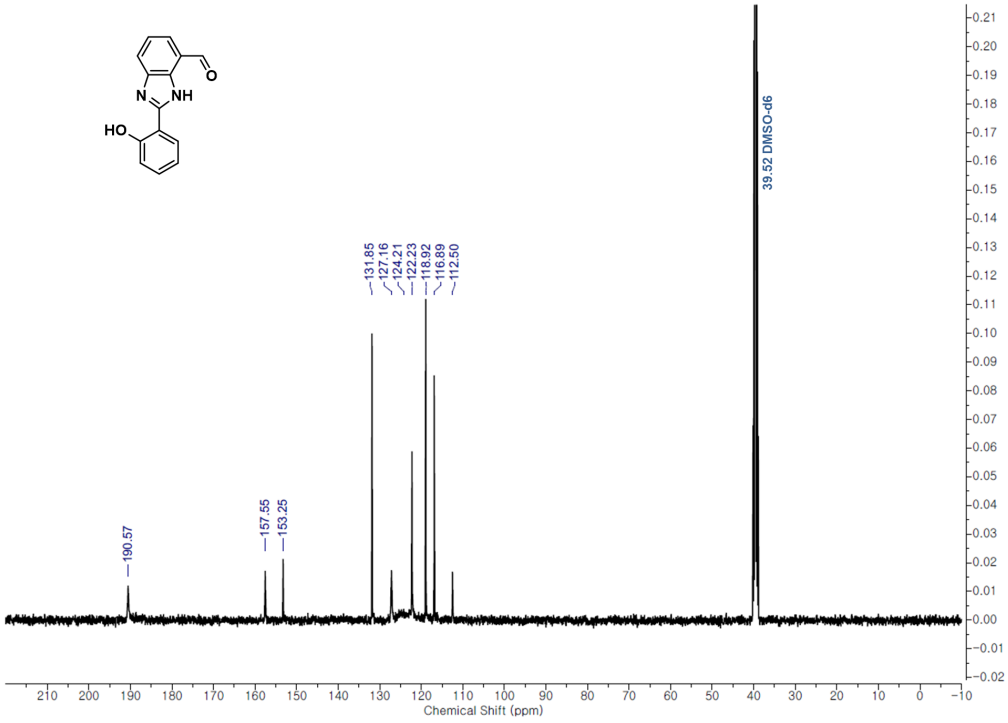

Fig. S26. ^{13}C NMR (100 MHz) spectrum of **3** in DMSO-d_6 (T = 343 K).

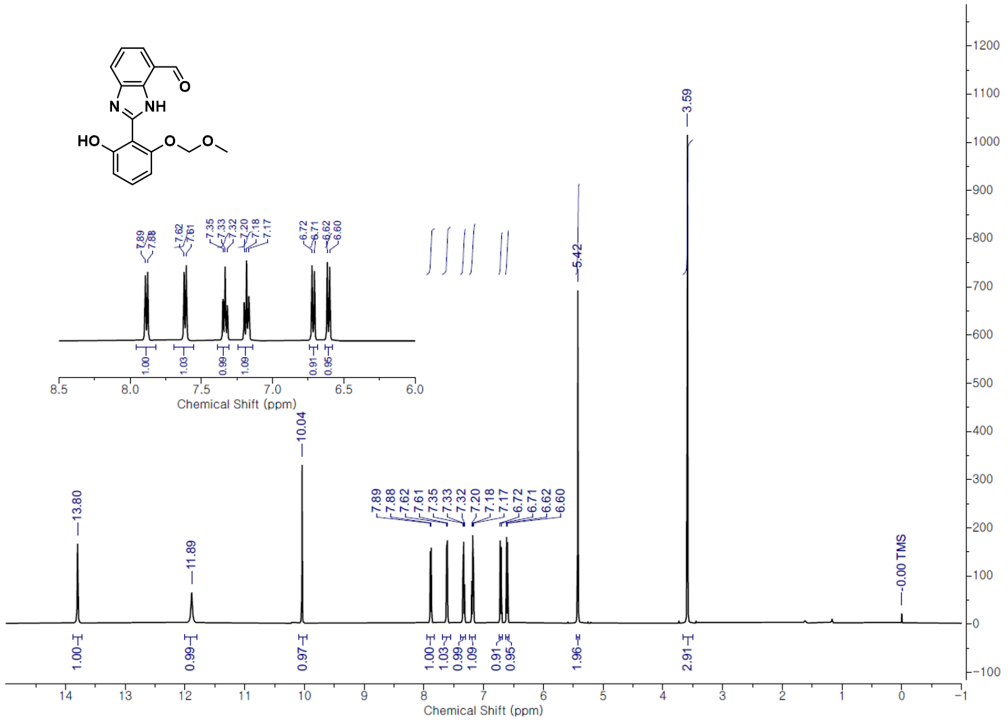

Fig. S27. ^{1}H NMR (500 MHz) spectrum of **4** in $CDCl_3$ (T = 298 K).

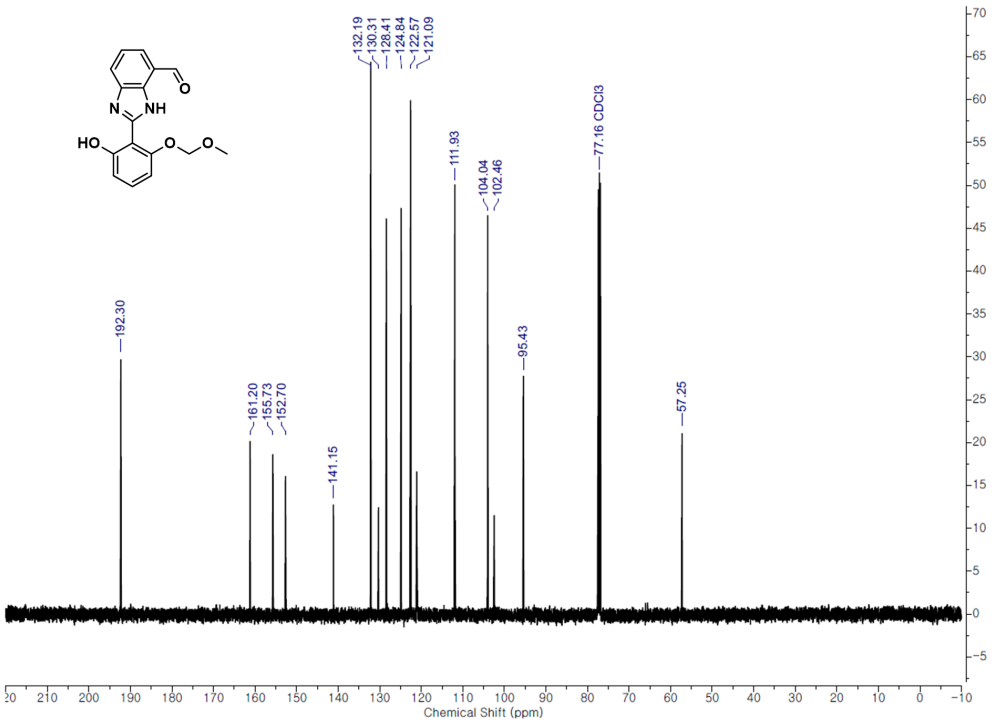

Fig. S28. ^{13}C NMR (125 MHz) spectrum of **4** in $CDCl_3$ (T = 298 K).

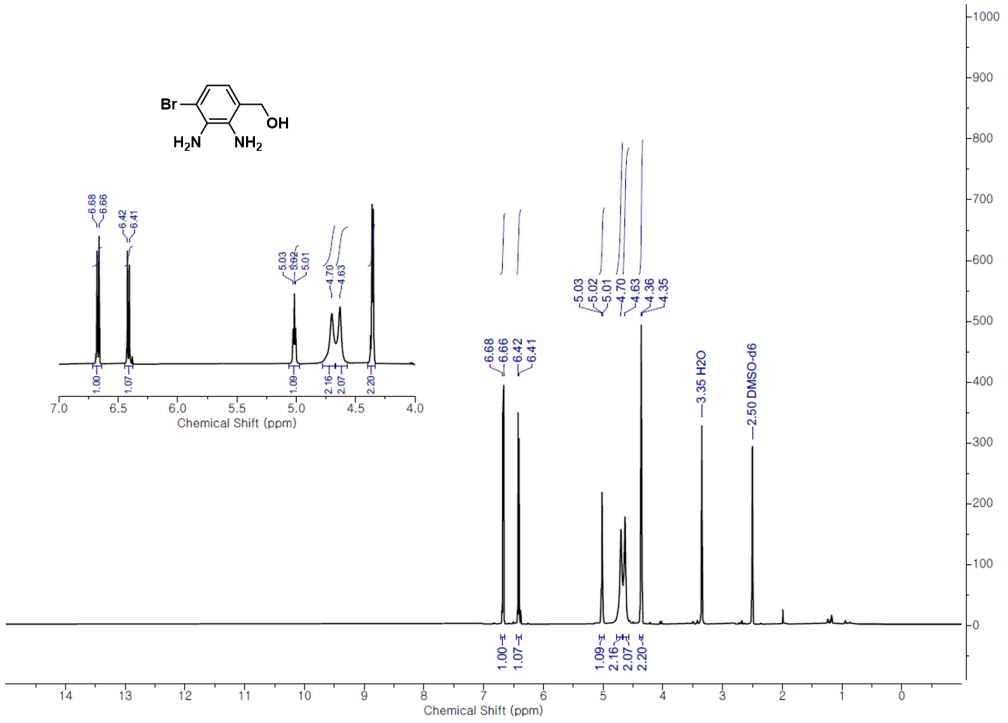

Fig. S29. ^{1}H NMR (500 MHz) spectrum of **10** in DMSO-d_6 (T = 298 K).

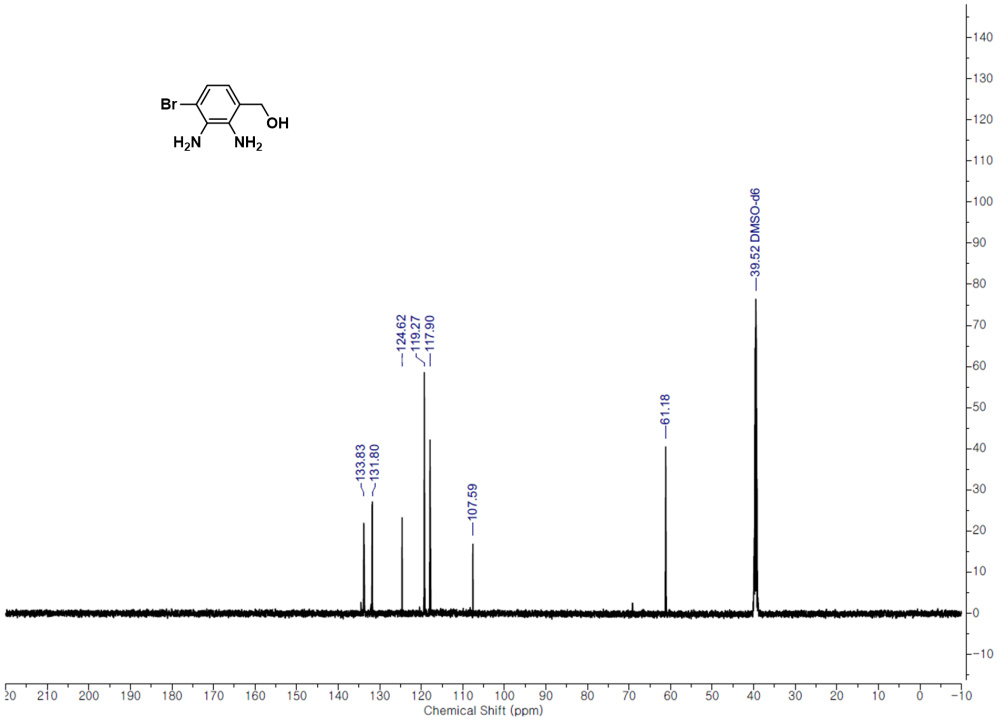

Fig. S30. ^{13}C NMR (125 MHz) spectrum of **10** in DMSO-d_6 (T = 298 K).

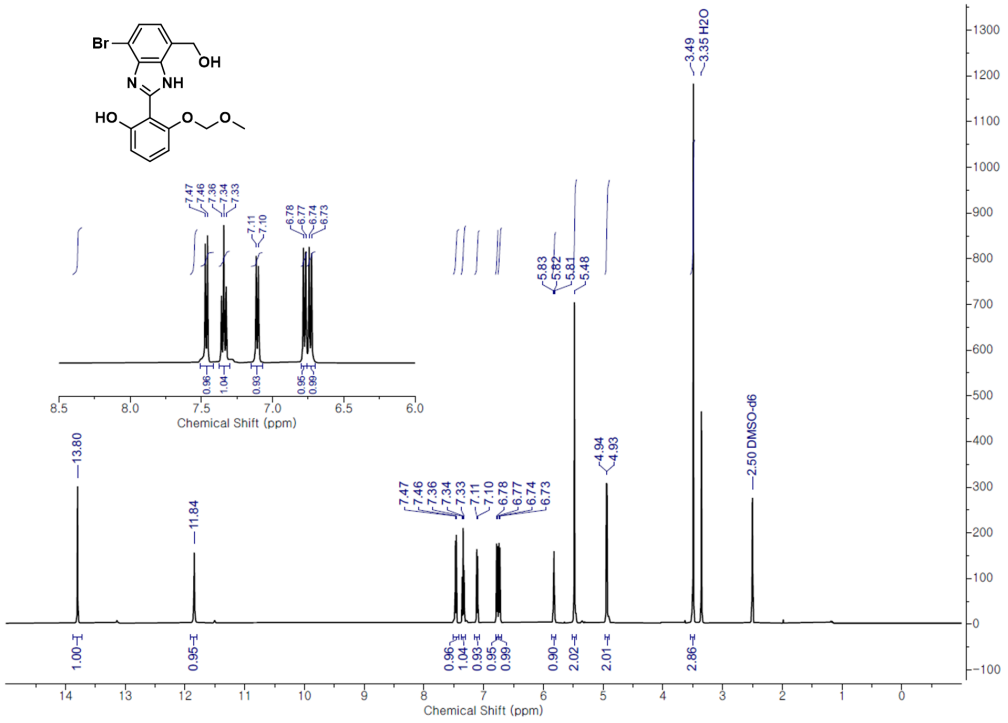

Fig. S31. ^{1}H NMR (500 MHz) spectrum of **11** in DMSO-d_6 (T = 298 K).

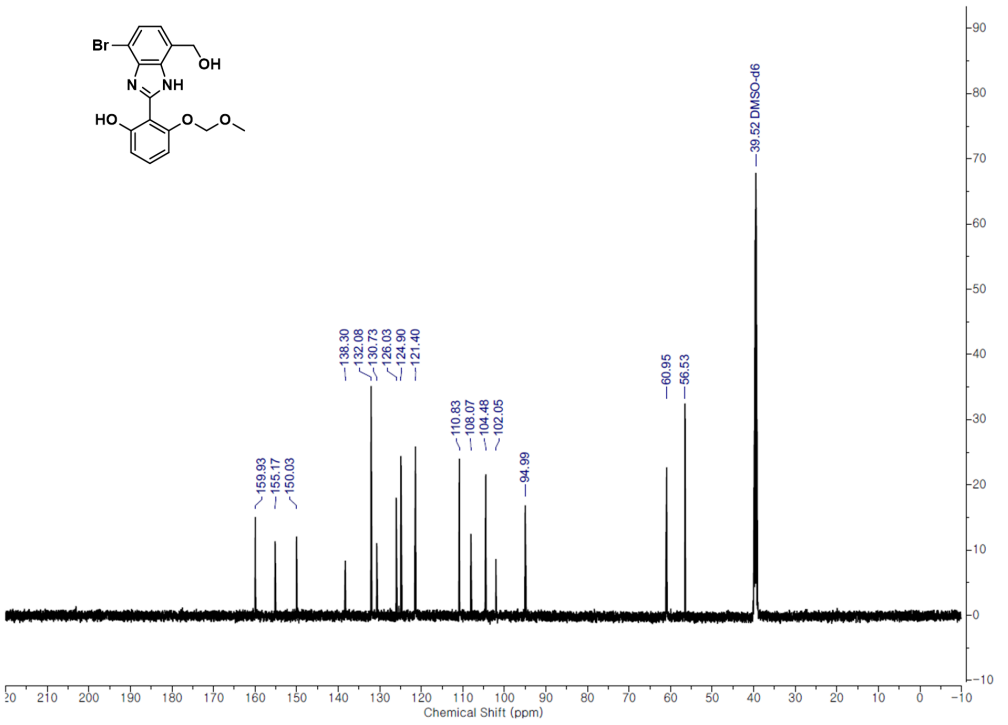

Fig. S32. ^{13}C NMR (125 MHz) spectrum of **11** in DMSO-d_6 (T = 298 K).

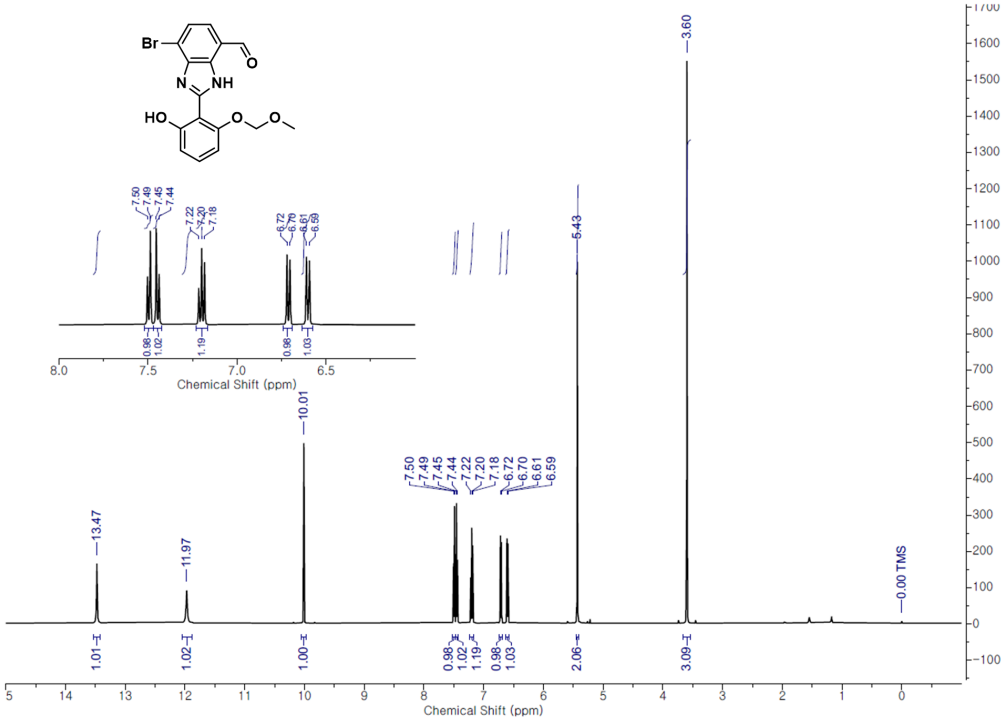

Fig. S33. ^{1}H NMR (500 MHz) spectrum of **6** in $CDCl_3$ (T = 298 K).

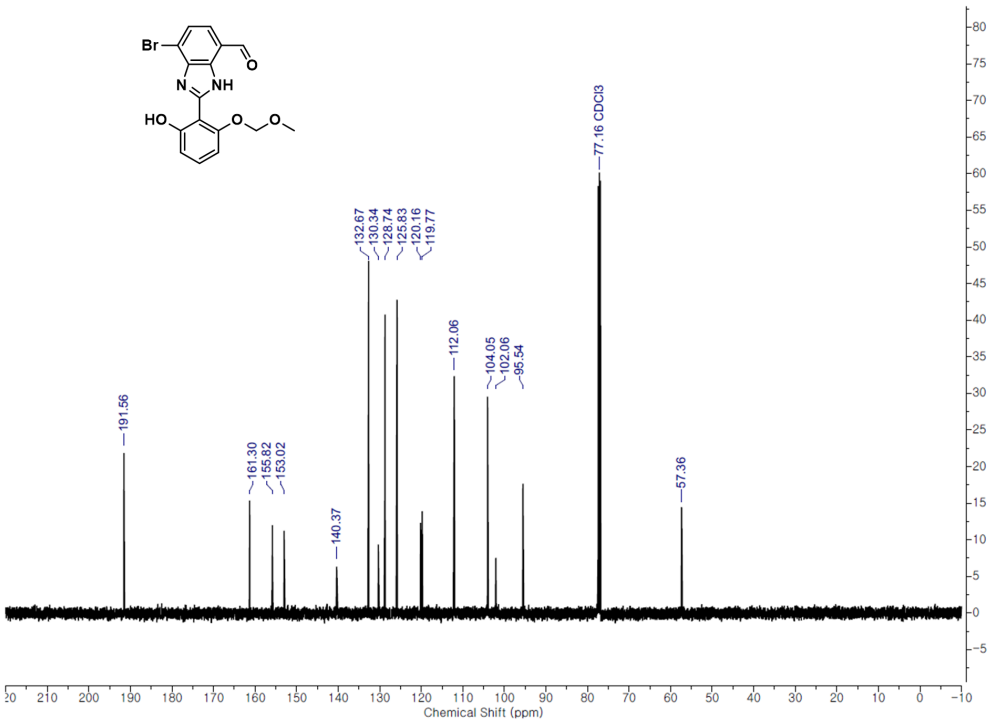

Fig. S34. ^{13}C NMR (125 MHz) spectrum of **6** in $CDCl_3$ (T = 298 K).

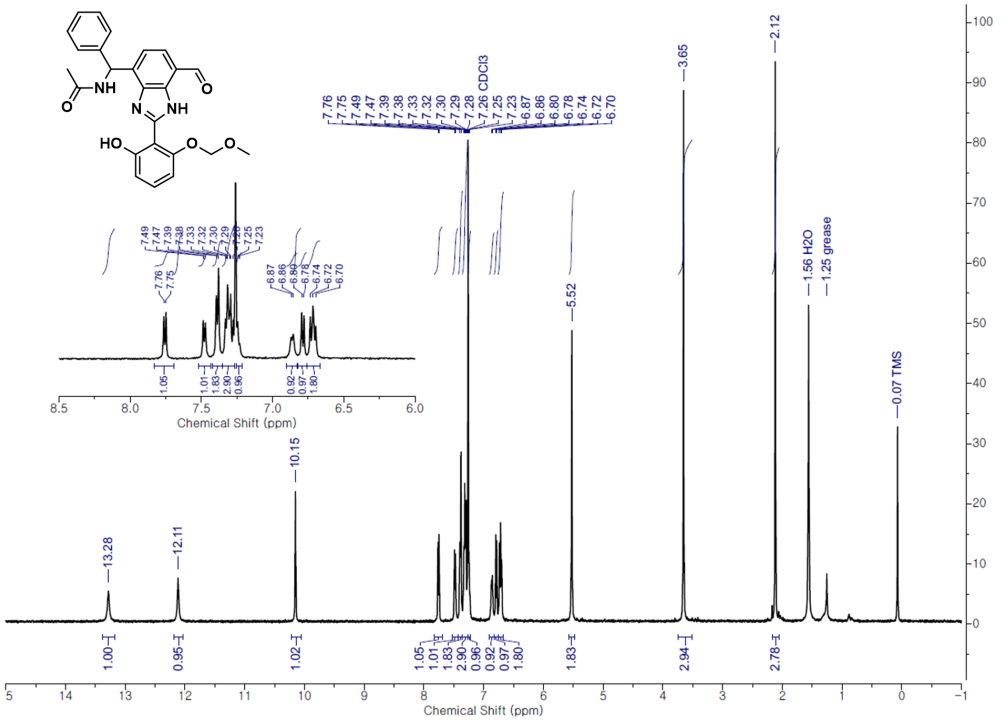

Fig. S35. ^{1}H NMR (500 MHz) spectrum of **1** in $CDCl_3$ (T = 298 K).

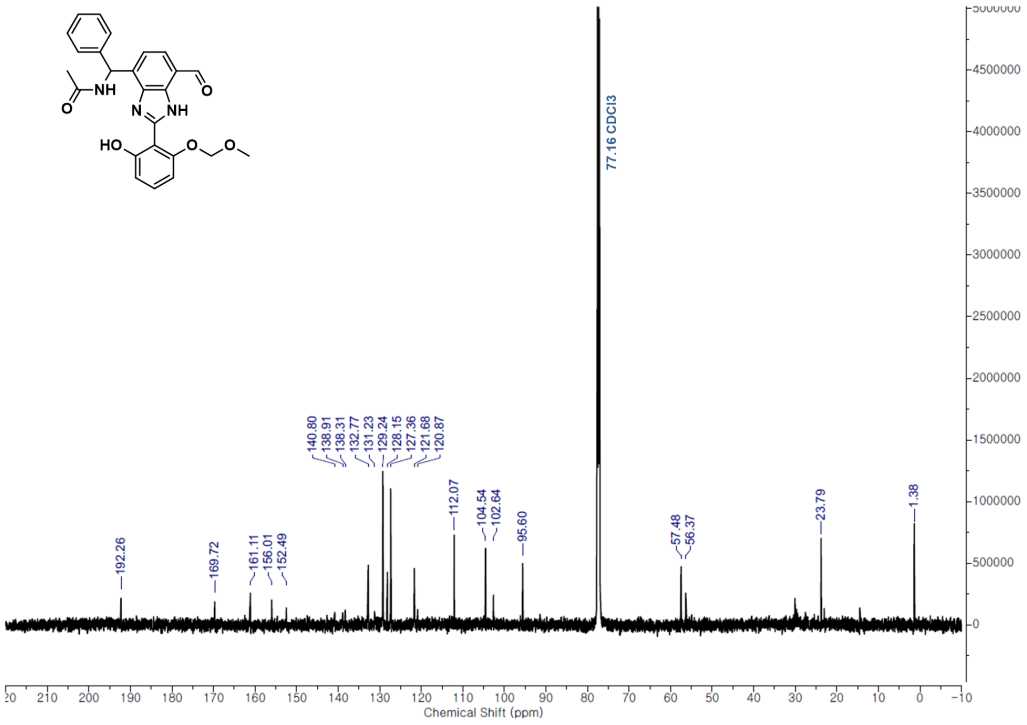

Fig. S36. ^{13}C NMR (150 MHz) spectrum of **1** in $CDCl_3$ (T = 298 K).